PLOS WATER

RESEARCH ARTICLE

Projection of irrigation water requirement in the south Mediterranean area using an explicit representation of irrigation processes into a land surface model: Case of the Tensift catchment (Morocco)

Ahmed Moucha[1,2], **Lionel Jarlan**[3*], **Pere Quintana-Segui**[4], **Anaïs Barella-Ortiz**[4,5], **Michel Le Page**[3], **Simon Munier**[5], **Adnane Chakir**[3,6], **Aaron Boone**[5], **Fatallah Sghrer**[7], **Jean-Christophe Calvet**[5], **Lahoucine Hanich**[1,8]

1 L3G Laboratory, Faculty of Sciences and Techniques, Cadi Ayyad University, Marrakech, Morocco, **2** Direction Générale de la Météorologie, Casablanca, Morocco, **3** CESBIO (Université de Toulouse/CNRS/INRAE/IRD/CNES), Toulouse, France, **4** Observatori de l'Ebre, Ramon Llull University - CSIC, Tarragona, Spain, **5** CNRM (Université de Toulouse/Météo-France/CNRS), Toulouse, France, **6** LMFE, Faculty of Sciences Semlalia, Cadi Ayyad University, Marrakech, Morocco, **7** ORMVAH-Office Régional de Mise en Valeur Agricole du Haouz, Marrakech, Morocco, **8** Geology and Sustainable Mining Institute (GSMI), Mohammed VI Polytechnic University (UM6P), Ben Guerir, Morocco

* lionel.jarlan@ird.fr

Citation: Moucha A, Jarlan L, Quintana-Segui P, Barella-Ortiz A, Le Page M, Munier S, et al. (2025) Projection of irrigation water requirement in the south Mediterranean area using an explicit representation of irrigation processes into a land surface model: Case of the Tensift catchment (Morocco). PLOS Water 4(2): e0000297. https://doi.org/10.1371/journal.pwat.0000297

Editor: Koffi Djaman, New Mexico State University, UNITED STATES OF AMERICA

Received: March 25, 2024

Accepted: December 8, 2024

Published: February 21, 2025

Data availability statement: In situ data were acquired within the frame of the TENSIFT observatory (https://www.lmi-trema.ma/observatoire/le-reseau-de-sites-de-mesure/) and are available upon request to Vincent Simonneaux (vincent.simonneaux@ird.fr) and Salah-Er Raki (s.erraki@uca.ma). SAFRAN forcing and

Abstract

In semi-arid areas, irrigation represents the largest human footprint on the water cycle. Representing irrigation in land surface and hydrological models is a challenging task as irrigation decisions depend on environmental, economic and traditional knowledge factors. The objective of this work is twofold: (1) to evaluate the performance of the new irrigation module integrated into the Interactions between Soil, Biosphere, and Atmosphere (ISBA) model and (2) to assess the future trajectories of agricultural water use considering both climate and land use change. The evaluation of the new irrigation module in the ISBA model is done by: (1) comparing the observed and predicted fluxes by the ISBA model, with and without the activation of the irrigation module, and (2) comparing the irrigation water inputs at the level of irrigated perimeters. The evaluation shows that the integration of the new irrigation scheme in ISBA significantly improves the latent heat flux (LE) predictions for the period 2004-2014, compared to the model without this scheme. Considering several flux stations, the LE flux bias was reduced from -60 W/m^2 for the model without irrigation to −15 W/m^2. The evaluation at the irrigated perimeter scale highlights the ability of the irrigation model to reproduce the overall magnitude and seasonality of observed irrigation water quantities despite a positive bias. The agricultural water use was then projected considering two climate scenarios and two scenarios of land use change based on the actual trend of conversion to tree crops in response to the large subsidy attributed for the conversion to drip irrigation since 2008. It is shown that (1) irrigation water use could almost double for the more extreme scenarios and (2) that most of this drastic increase is attributed to land use change, including irrigation

future scenario (doi: 10.5281/zenodo.1383886) are available at the following URL: https://doi.org/10.5281/zenodo.13838861

Funding: This work was partly funded by FP7 ERANET-MED CHAAMS, H2020 PRIMA IDEWA and RISE-H2020 ACCWA projects.

Competing interests: The authors have declared that no competing interests exist.

intensification and expansion. Within this context, the results presented in this study highlight the side effect of conversion to drip irrigation largely documented in the literature and open perspectives for making informed decisions for sustainable water management at the watershed level.

Introduction

The southern Mediterranean region is characterized by limited water resources and periods of water scarcity due to recurring droughts [1] that may be exacerbated by future warming and precipitation decrease associated with climate change [2]. About 70% of available resources are used worldwide by the agricultural sector through irrigation with strong regional discrepancies ranging from less than 20% in northern Europe up to 90% in some south Mediterranean countries [3]. Food security and the economy of the south Mediterranean countries largely rely on irrigated agriculture. In Morocco, 19% of arable lands are irrigated and sustain the livelihood of 40% of the agricultural labour force and produce 45% of the added value in the agricultural sector [4]. The projected reduction of available surface water resources [5] may severely impact the agricultural sector by enhancing the inter-sector competition [6,7]. As a result of the decline in surface water and easier access to groundwater through boreholes (which are often neither registered nor monitored), groundwater is under increasing pressure exceeding the recharge rate and leading to groundwater depletion [8–10] in the order of one to two meters per year in some regions, with complete depletion in some places [11]. With population growth, rising incomes, and changing diets, irrigation water demand is likely to increase through the intensification of already cultivated land and the expansion of irrigated area [12]. Despite these key societal issues for human well-being, irrigation water demand remains highly uncertain [13,14] threatening the implementation of sustainable water management strategies.

Saadi et al. [15] showed that the net irrigation requirements for optimal water supply in the southern Mediterranean region could decrease by 11% by the year 2050, in response to the shortening of the growing season associated with temperature increase. However, most studies have highlighted a potential increase in irrigation water in the future. [16], based on a multimodel ensemble, projected a 25% increase in irrigation water demand by the end of the century and for the RCP8.5 scenario. Indeed, the increase in evaporative demand due to higher temperatures [5] cannot be offset by the reduction in growing season length and stomatal closure [4] as shown by [17]. Similarly, [18] found a strong increasing trend of irrigation water demand in the Mediterranean region, associated with the effect of warming on evaporative demand. In addition to climate change, some authors also attempted to account for the ongoing land use change in the region. In response to incentive public policies that promote the conversion of traditional irrigation techniques to drip irrigation, a strong trend of change from traditional crops such as cereals to tree crops can already be observed in the region [19,20]. Proposed an empirical method for projecting irrigation water demand, taking into account these already initiated processes of large-scale land use change. They highlighted that the irrigation supply could almost triple by 2050 under the RCP8.5 scenario over the Tensift basin in Morocco. In the Iberian Peninsula, for example, a significant increase in water demand is also projected by several studies [21,22]. Similarly, [23] suggest a significant increase in gross irrigation, which could reach 74% in the more extreme scenarios.

Beyond projecting irrigation water demand to assess the sustainability of irrigated agriculture and to develop adaptation strategies, irrigation significantly impacts the hydrological

cycle, the thermo-hydric properties of the atmosphere, and potentially precipitation patterns. Indeed, in semi-arid regions, irrigation creates contrasting soil moisture conditions between the irrigated areas and the surrounding hot and dry areas. This cools and wets the atmosphere downwind of irrigated areas [24], locally affects the partitioning of available energy into sensible and latent heat fluxes [25,26], promotes sensible heat advection [27], and affects the dynamics of latent heat fluxes by favoring plant transpiration at the expense of soil evaporation, thereby enhancing the land-atmosphere feedback [28]. These processes have been shown to affect precipitation patterns [29]. The expansion and intensification of irrigated areas worldwide have motivated the scientific community to develop measures to better understand the land-atmosphere feedback processes over irrigated areas [30]. Despite the importance of being able to account for irrigation in land-atmosphere studies, irrigation and anthropogenic water management in general are still poorly represented in land surface models (LSMs), which provide the lower boundary for the atmosphere in global circulation models [25,31].

A realistic representation of irrigation processes in global LSMs is a real challenge (Wada et al. 2017) [32], as they should be able to represent irrigation quantity and frequency, irrigation technologies, and the decision process that triggers water supply. Other LSMs embedded in land data assimilation systems (LDAS) account for irrigation by assimilating surface soil moisture products and/or Leaf Area Index (LAI) derived from remote sensing observations, which correct for the shortcomings of the modeling approach [33,34]. To project the future impact of irrigation on climate, some LSMs explicitly represent irrigation but are limited to one type of irrigated crop associated with one irrigation technology such as the ISBA model [35,36], which can only irrigate C4 crops with the sprinkler technique, whereas all crops worldwide can be irrigated with a wide variety of techniques that deliver water above or below the canopy, with important implications on irrigation efficiency and on soil-vegetation-atmosphere water fluxes. In recent years, some more generic irrigation schemes have been developed and incorporated into LSMs [37,38], developed a human water management model including dam regulation and irrigation practices, which was tested with the ORCHIDEE model in the Yellow River basin using streamflow observations. [39], incorporated an irrigation scheme into the NOAH-HMS model, which was evaluated in the Yangtze River basin against streamflow data, GLEAM evapotranspiration products [40], and irrigation statistics. [41] also proposed an irrigation scheme coupled to the ISBA model embedded in the SURFEX modeling platform, and they indirectly tested the added value of irrigation representation compared to satellite observations. However, most of these studies often lack direct irrigation observations to assess the quality of irrigation predictions while irrigation information derived from remote sensing still lacks accuracy [42].

Therefore, good monitoring and future projection of irrigation water supply is of paramount importance for implementation of sustainable water management strategies and for food security, as well as for the improvement of weather and climate predictions. In this context, the objective of our study is twofold: (1) to assess the performance of the new irrigation scheme developed by Druel et al. [41] in the ISBA model on a semi-arid catchment located in the region of Marrakech (Morocco), where irrigation observations were collected; (2) to assess the future demand for irrigation water taking into account both climate change and land use change.

Materials and methods

The overall approach is summarized by the scheme in Fig 1. The different data sets, the model including the irrigation module, and the implementation are described in the following sections.

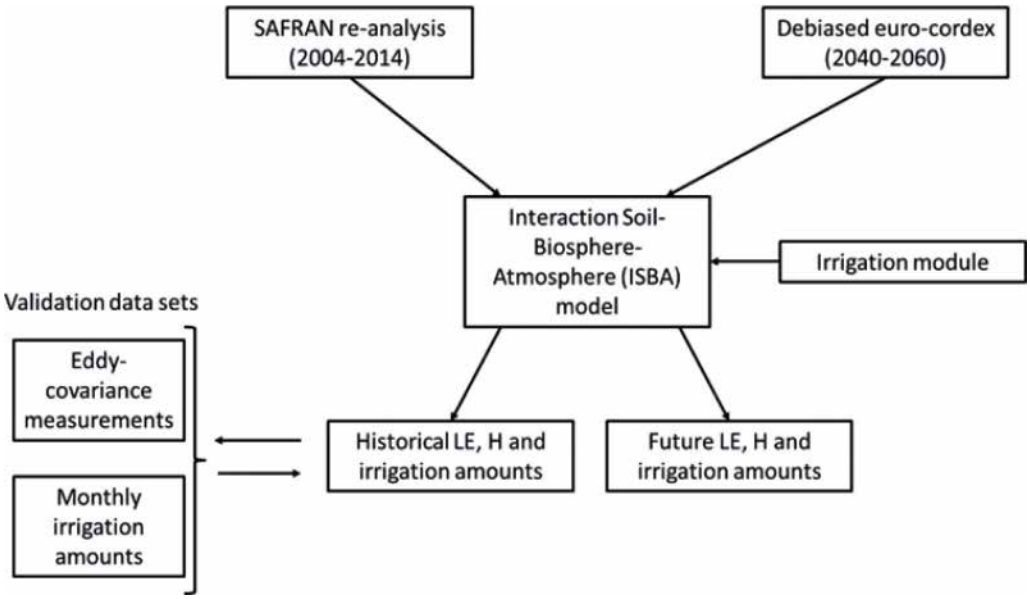

Fig 1. Summary of the approach.

https://doi.org/10.1371/journal.pwat.0000297.g001

Study region and data

After a brief description of the study area, several datasets are detailed. Some were used for the validation of the land surface model (evapotranspiration measurements, irrigation water amounts) and the others (SAFRAN meteorological forcing, land cover map) were used as inputs to the model.

Study area. This study was carried out on the Tensift watershed, located in the Marrakech region of Morocco. The Tensift is considered a representative example of many anthropized basins in the South Mediterranean region. The Tensift basin covers an area of 19.800 km^2, among which 3.100km^2 are used for irrigated agriculture [12,43]. The climate is semi-arid to arid, governed by the complex orography of the High Atlas Mountains and western flows bringing humid and cold air from the Atlantic Ocean. The basin is divided into two zones that present a contrasting hydrological functioning: the southern part of the Tensift basin, located on the north slope of the High Atlas, has average annual precipitation between 600 and 700 mm/year and contributes to the support of base flows during the summer thanks to the melting of snow stored in winter [44]. The Haouz plain to the west is dedicated to intensive irrigated agriculture mainly composed of cereals, olive, citrus, and market gardening, and receives an annual precipitation ranging between 200 and 400 mm/year.

The surface of the Tensift watershed basin is composed of four main categories of soils. The first is a grayish soil, typically found in the lower parts of the oueds in the central Haouz area. The second category is a chestnut-colored soil, located mainly at the boundary of the eastern Haouz and along the Rocade canal in the central Haouz. The third category is a reddish-chestnut soil, developed on cemented gravel or limestone, found at the southern limit of the central Haouz and in the central zone of the eastern Haouz. The fourth category is a brown soil with a gravelly or lamellar crust, sometimes calcareous, found along the reliefs of the Jbilets and north of the central Haouz. These four types of soils, in combination with a Mediterranean climate, allow for the growth of a diverse range of vegetation in the Tensift watershed basin.

The crops are irrigated using water from dams, direct diversions from the river beds, as well as water extracted from the underlying aquifer with an exponential increase in the number of private drillings during the last 10 years outside any legal framework [19]. The so-called modern irrigated perimeters reported in Fig 2 are fed by either dams or by water transfer from the Sebou catchment to the north.

Water is then conveyed by gravity through a hierarchical network of concrete overhead channels. The modern irrigation districts are managed by the agricultural water management agency called the Regional Office for Agricultural Development of Haouz (ORMVAH). Since the 2000s, this area has been the subject of meteorological, micro-meteorological, and hydrological monitoring as part of the Tensift Observatory jointly led by the Cadi Ayyad University of Marrakech and the French Institute for Sustainable Development through the CESBIO and HSM laboratories.

Present and future meteorological forcing. The SAFRAN re-analysis system [45] was implemented on the Tensift catchment to map the main meteorological variables (air temperature and humidity, wind direction and speed, surface atmospheric pressure, short and long wave incoming radiation and liquid and solid precipitation) during the 2004–2014 period. SAFRAN is based on an optimal interpolation between a forecast (the weather forecast

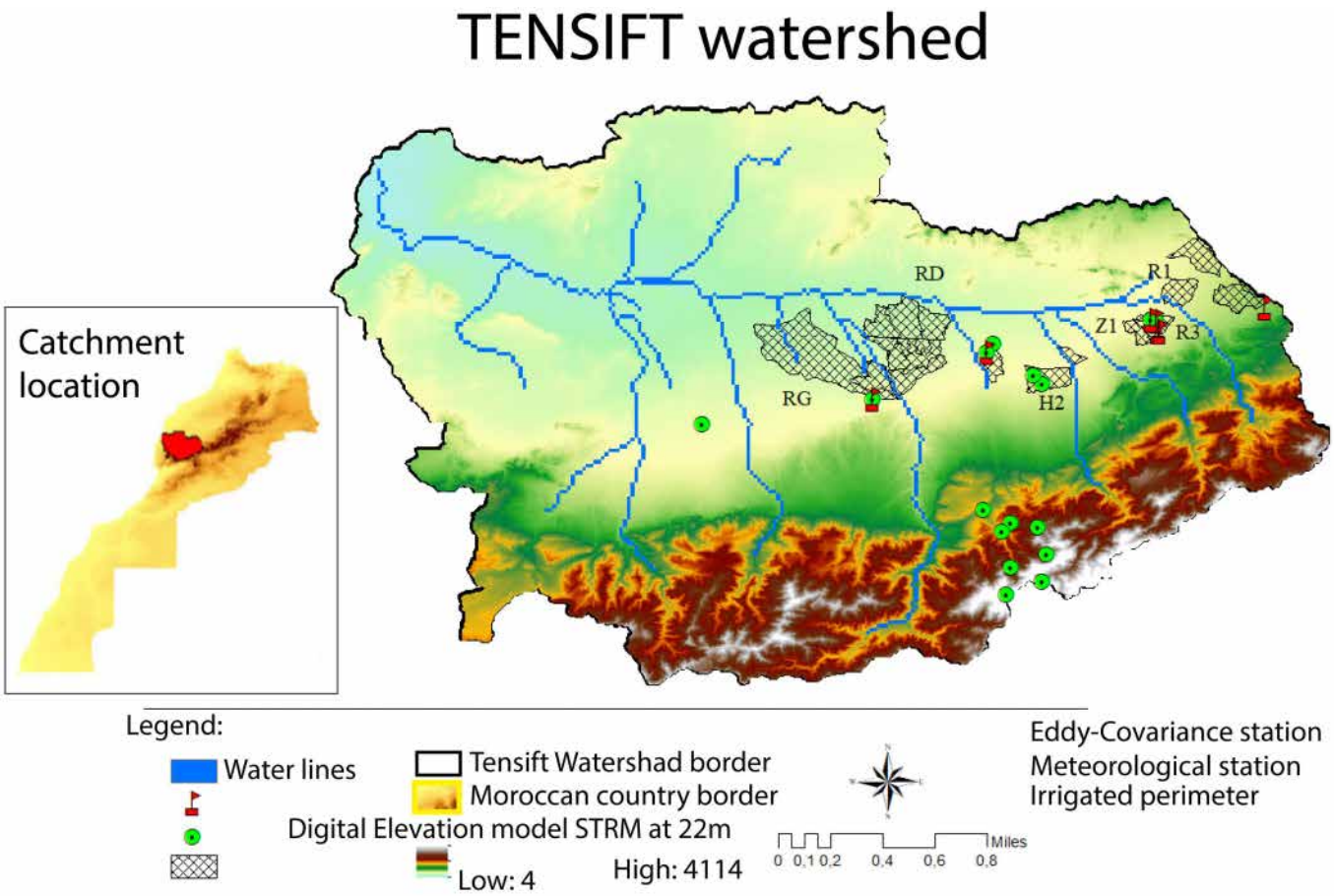

Fig 2. The Tensift catchment and the orography (digital elevation model STRM at 22m). The location of Eddy-Covariance and meteorological stations and also irrigated perimeter. All the border shapes are provided by openstreemap (https://www.openstreetmap.org/) under the Open Data Commons (ODbL) licence (https://opendatacommons.org/licenses/odbl/summary/).

https://doi.org/10.1371/journal.pwat.0000297.g002

system used operationally by the Moroccan Metoffice in this study) and observations (data from 18 meteorological stations were used). A variable grid with grid point dimensions ranging from 1 km^2 to 8 km^2 was used to better represent orography and irrigated perimeters. In other words, a resolution up to 1 km^2 was applied on mountainous areas and irrigated districts.

The future projection of precipitation and temperature is based on the EURO-CORDEX ensemble [46] at 12 km resolution that was downscaled (i.e., debiased) using the SAFRAN re-analysis based on a combination of the quantile-quantile approach [47] and a delta change method [48]. A total of four regional climate models were used (CNRM, KNMI, IPSL and MPI) to compute changes and two scenarios (RCP4.5 and RCP8.5) were selected for the projection of temperature and precipitation at the 2041–2060 horizon (median of the four regional climate models). The present and future climate forcing are described and analyzed in details in [49].

Convective flux observations. A series of experiments were conducted aiming to measure the terms of the surface energy budget, including the convective latent (LE) and sensible (H) heat fluxes of the main crops of the region in the Haouz plain since 2002 within the frame of the Tensift observatory. The eddy covariance stations were installed on irrigated areas (Agafay, Agdal, R3, and Saada) sampling olive, citrus, and wheat and also on rainfed wheat (named Bour). All the available data sets are described in Table 1 and reported in Fig 2. The stations were composed of a Krypton hygrometer (model KH2O—Campbell Scientific Inc., Logan, UT, USA) or a Licor analyzer (open-path Li-7500 or closed-path Li-7200 depending on the station) measuring the water vapor at a rate of 20Hz and a 3D sonic anemometer (CSAT3, Campbell Scientific Ltd.) measuring the wind speed at high frequency. Half-hourly fluxes of LE and H were calculated through post-processing of the 20Hz raw data using Edipro Software for Licor data and ECPACK Software for KH20 data. Considering the scale mismatch between the model grid point dimension (>= 1 km^2) and the footprint of the eddy-covariance (~100 m^2) together with the irrigation timing and amount predicted by the model that would be different from what was really applied to the field by the farmer, a perfect match between predicted and observed LE was not expected. Within this context, no budget energy closure method [50] was applied to the data. Most of the data sets have been extensively used and described in several studies [51–55].

Water supply. Monthly irrigation water amounts at the scale of some irrigated perimeters were provided to assess the performance of the model for the irrigation amount prediction, particularly their monthly and interannual variabilities. They were provided at the monthly timescale by our partner in charge of the management of the agricultural water from 2004 to 2014. The considered irrigated perimeters are reported in Fig 2. Only surface water coming

Table 1. Characteristics of the eddy-covariance stations used for the evaluation of convective fluxes.

Eddy-covariance stations	Latitude (°)	Longitude (°)	Elevation (m)	Time Period	Crop
Agafay	31.496	−8.228	506	2006–2010	Citrus
Agdal	31.601	−7.974	479	2004–2005	Olive
Bour	31.701	−7.352	730	2013–2014	Rainfed wheat
R3	31.673	−7.596	593	2007–2009, 2010–2013	Irrigated wheat
R3 Olive	31.67	−7.6	590	2006–2007	Olive
R3 North	31.649	−7.589	587	2012–2014	Irrigated wheat
R3 South	31.648	−7.588	589	2012–2014	Irrigated wheat
Saada	31.673	−7.607	415	2004–2006	Olive

https://doi.org/10.1371/journal.pwat.0000297.t001

from dams or extracted from the transfer channel coming from the northern catchment was officially registered and considered when comparing with model data. However, several farmers, in response to the early 2000s drought, have drilled boreholes to supplement the agricultural office's water allocation. Indeed, drinking water is obviously given priority in the water management scheme of the catchment and the remaining water is allocated to the other sectors including agriculture once drinking water needs are satisfied. This means that water amounts allocated to farmers are usually far from reaching the optimal crop water needs. In addition, tree crops are given priority over annuals and in case of severe water shortage such as in the recent years of 2020 and 2021, no water is allocated to annuals. Unfortunately, no data was available for the wells, meaning this water source was not accounted for in data comparisons.

Land cover map and static inputs for the land surface model. The land cover map used as input for the SURFEX platform was ECOCLIMAP Second Generation [56], hereafter referred to as ECOCLIMAP. It is composed of 33 surface land covers among which 17 are crops or natural vegetation functional types. In this study, wheat was associated with the vegetation functional type "C3 crops", and olive and citrus to "temperate broadleaf evergreen". Together with the land cover map, a 2008–2012 climatology of albedo [57] and Leaf Area Index [58] at 300 m resolution was used as input to the land surface model in this study. They are derived from the dataset provided by the Copernicus Global Land Service based on Proba V data. The soil texture used to compute the soil hydrodynamic characteristics (Wilting point, field capacity and saturation) using the pedo-transfer function of [59] was derived from global Soil grids.

Following the development of the irrigation module in the ISBA LSM [41], the irrigation map of Meier et al. [60], was used to locate the potentially irrigated areas. Meier's map was based on national statistics and remote sensing data gathered during the 1999–2012 period. Nevertheless, considering the potential strong uncertainties of this global irrigation map, some changes were applied to better fit local irrigation conditions: (1) on the modern irrigated perimeters shown in Fig 2, irrigation was turned on for the whole area (Fig 3); (2) the ECOCLIMAP-SG was updated to take into account the ongoing strong mutation of agriculture in the region. Indeed, agriculture has undergone major changes, especially since the implementation of the "Green Morocco" program in the late 2000s, which heavily subsidized the conversion from traditional flood irrigation to drip irrigation. This transformation has had a significant impact on water consumption: farmers have mainly abandoned wheat cultivation in favor of tree crops, which require irrigation throughout the year. They have also expanded their irrigated areas thanks to increased access to water, thus facilitating irrigation of neighboring fields that were originally not irrigated. The number of wells has also increased significantly, as it is easier to use drip irrigation with groundwater than with surface water. In response to this tendency of conversion from cereals to tree crops, annual land use maps separating annuals (i.e., cereals) from tree crops were computed from the 250m MODIS NDVI and a decision tree approach using the thresholds proposed by [20] and [61]. A majority filter was then applied to provide a land use map representative of the period of study and pixel identified as trees in the MODIS land use map were turned to "temperate broadleaf evergreen" in the modified version of ECOCLIMAP-SG and irrigation was also turned on for these grid points. Fig 3 displays the new version of ECOCLIMAP-SG on the Tensift catchment.

Finally, as most new plantations of tree crops use drip irrigation thanks to the incentive policy financing a large part of the equipment, it was assumed that all tree crops are irrigated using the drip technique. By contrast, wheat crops were assumed to be irrigated by the traditional flooding technique.

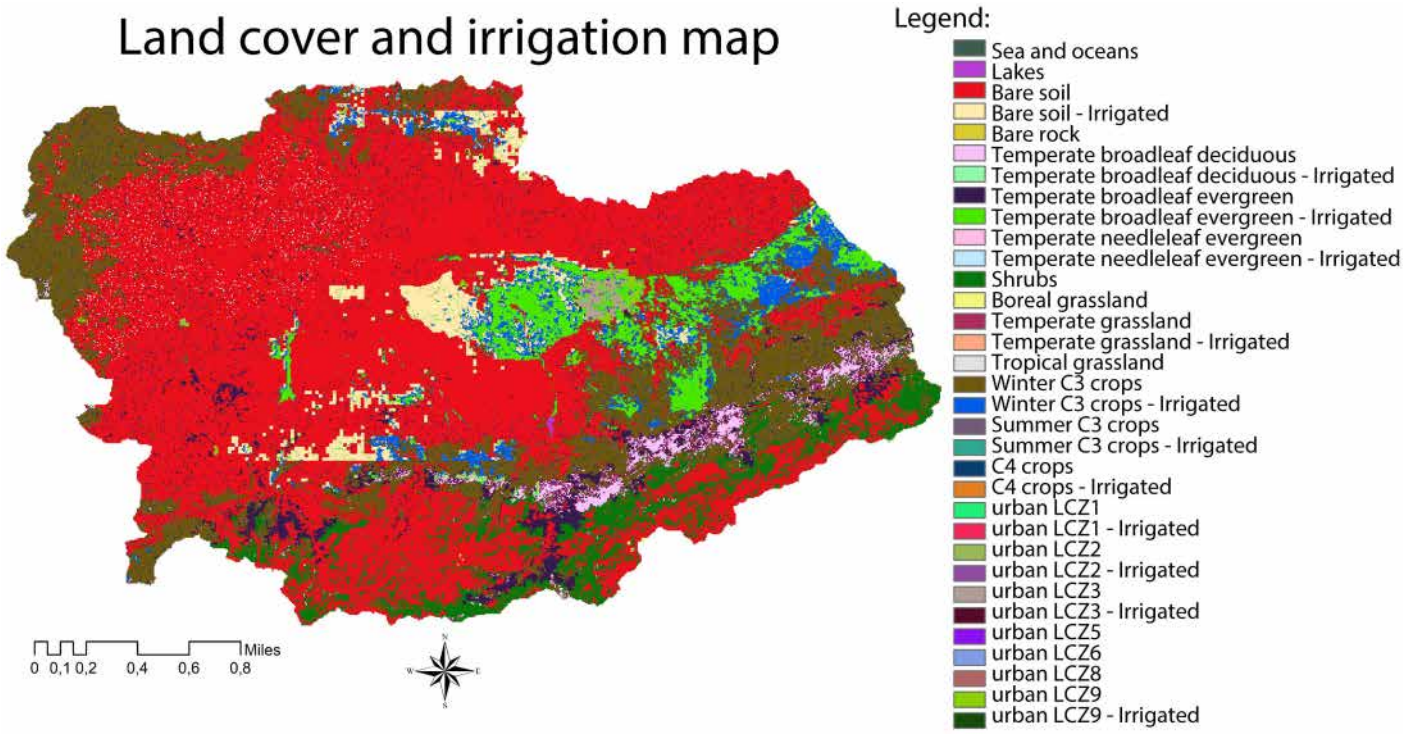

Fig 3. Land cover and irrigation map modified from ECOCLIMAP second generation (see text). All the border shapes are provided by openstreemap (https://www.openstreetmap.org/) under the Open Data Commons (ODbL) licence (https://opendatacommons.org/licenses/odbl/summary/).

https://doi.org/10.1371/journal.pwat.0000297.g003

Model and implementation

The ISBA land surface model. The ISBA LSM [62,63], which is a composite soil-vegetation land surface scheme that simulates surface energy exchanges within the soil-vegetation-atmosphere continuum, is an embedded component of the SURFEX platform [64]. In this study, the ISBA-A-gs scheme [65,66], which couples the ISBA model with a net CO2 assimilation (A) - stomatal conductance (gs) appoach (A-gs) was used. ISBA-A-gs takes into account the functional relationship between net CO2 assimilation and stomatal aperture at the leaf level, and employs the physiological parameterization of stomatal conductance as proposed in [67] to describe plants' photosynthesis. For this study, the non-interactive vegetation option was selected, which implies that vegetation characteristics such as leaf area index, fractional cover, and vegetation height were prescribed using the climatological data sets described in the previous section. The solar radiation transfer scheme employed a multi-layer configuration that accounted for both sunlit and shaded leaves [68]. The soil's transfers and heat exchanges were simulated using the multi-layer soil diffusion scheme [69,70], which was found to perform better on crops [71] than the previously implemented force-restore approach [72].

Irrigation module. In response to the urgent need to represent agricultural practices in global land surface models to better represent the water cycle of anthropized catchments, [41] proposed an irrigation scheme that can be easily parameterized to fit all irrigation techniques. This scheme has been available since version 8.1 of the SURFEX platform. The irrigation scheme can simulate sprinkler irrigation, flood irrigation, and drip irrigation. For flood and drip irrigation, water is applied directly to the soil surface, bypassing canopy

interception. Irrigation was applied from emergence until two weeks before harvest. Irrigation was triggered when the soil water index (SWI) fell below a threshold that changed throughout the growing season: 0.7 for the first irrigation, 0.55 for the second, 0.4 for the third and 0.25 for the fourth, based on [35] and [36]. The irrigation amounts were set by the user and applied when the SWI indicates water stress, during daytime hours from 8 am to 8 pm. A minimum time period between two irrigation events could be constrained to mimic irrigation systems that deliver water to the field with a network of canals (i.e., a water turn).

Implementation

The ISBA model was run on the Tensift catchment using the modified land cover and irrigation map derived from ECOCLIMAP Second Generation on the variable grid scale with grid point sizes ranging from 1 to 8 km of the SAFRAN re-analysis for the 2004–2014 period. Soil hydraulic characteristics were computed from clay and sand content of the Harmonized Soil Data Base from FAO [73] using the pedo-transfer functions of [59].

For the historical period, two experiments were conducted aiming to assess the added-value of irrigation representation: (**EXP1**) didn't consider irrigation while (**EXP2**) included irrigation. The parameters of the irrigation module are reported in Table 2. Trees are mainly cropped on private farms equipped with their own drilling, meaning they have access to water on-demand: the return time between two irrigation events was low (2 days). By contrast, wheat is mainly irrigated through flooding and cropped on irrigated perimeters: irrigation is organized by water turn meaning a constrained time between two irrigation events (about 10 days). Likewise, low irrigation amounts were considered for drip irrigation (5mm) while more water is needed for the fields to be completely watered (60 mm). Wheat is usually cropped in winter (seeding time is about mid-November and harvest occurs around mid-May). The predicted sensible and latent heat fluxes at the daily scale of EXP1 and EXP2 were then compared to the observations data considering the nearest grid point. Finally, irrigation water amounts predicted by the model for EXP2 were also compared to the water amount delivered by ORMVAH on some irrigation perimeters where data were available at the monthly time scale.

For the prediction at the 2050 horizon, 6 experiments combining 3 scenarios of land use change with the two climate scenarios RCP4.5 and RCP8.5 were carried out aiming to

Table 2. Parameters of the irrigation module.

	Vegetation type	EXP2
Irrigation frequency	Tree	2 Days
	Wheat	20 Days
Irrigation type	Tree	Driping
	Wheat	Flooding
Water supply	Tree	5mm
	Wheat	60mm
Irrigation time	Tree	12h
	Wheat	
Seeding date	Tree	01-August
	Wheat	15-Nov
Reaping date	Tree	30-Jul
	Wheat	10-May

https://doi.org/10.1371/journal.pwat.0000297.t002

unravel the effect of climate change on irrigation water supply from the impact of the change of agricultural practices. The three scenarios of land use change were as follows: (Historical) considered the same land cover and irrigation map of the historical period meaning the partition of trees and annuals was the same as for the 2004–2014 period; (Baseline) introduced a projection of the tree fraction at the pixel scale. To this objective, an empirical projection of the tree cover fraction was implemented following [20]. These authors developed an empirical approach to project the crop coefficient Kc of the FAO-56 single coefficient method to estimate crop evapotranspiration [74]. This method is based on the observed linear trends of MODIS NDVI taken as a proxy of Kc during the 2001–2020 period and corrected annually by the rainfall amounts to consider climate interannual variability. On a mixed grid point composed of both trees and annuals, Kc exhibits a seasonal cycle with the lowest value observed in summer when winter wheat is already harvested, and wheat fields are bare. This lowest value corresponds to the Kc of the trees. The fraction of trees was then derived from the linear trend of this summer Kc value. While a negative trend was observed on the coastal areas probably in response to the regression of argan forests [75], most of the region was subject to a drastic increase of tree crops. It is important to keep in mind that extrapolating the observed linear trend was a very extreme scenario of conversion to tree crops and will not be sustainable considering the available water resources, in particular, groundwater. It is thus very probable that the conversion will undergo an inflexion in the following years. (Inflexion) was thus the baseline scenario of conversion with an inflexion aiming to limit the conversion. Fig 4 displays the cover fraction of trees for the historical period and for both scenarios (baseline and inflexion) at the 2050 horizon.

Results

The results section is organized as follows: the first part is dedicated to the assessment of the prediction of latent heat fluxes and the irrigation water amounts during the historical period from 2004 to 2014, while the second part aims to analyze the irrigation water predictions on a seasonal and interannual time scale, as well as to analyze the future projections.

Evaluation of the irrigation scheme

Latent heat fluxes. Predictions of latent heat fluxes and irrigation water amounts by the model with and without the irrigation scheme activated are presented at Figs 5 and 6 for two seasons of tree crops and two seasons of wheat taken as representative examples (rainfall events were superimposed on irrigation water supplies for comparison purposes). In addition, all the time series of H and LE are provided as supplementary material in S1 Fig and S2 Fig.

Table 3 reports the statistical metrics (bias, RMSE and correlation coefficient r). Thanks to the activation of the irrigation module, the bias between the predictions and the eddy-covariance measurements was drastically reduced for all crops. Considering all the stations, the underestimation of LE without irrigation was about −60 W/m^2. It was significantly improved with the representation of irrigation (−15 W/m^2). The major impact for trees is during summer when the evaporative demand was the highest (see for instance Fig 5). The correlation coefficient was also considerably improved, meaning that not only did the irrigation module succeed in reducing the bias, but it was also beneficial to the prediction of the dynamics of LE. For instance, over Saada (Fig 5A), the correlation coefficient increased from −0.14 to 0.79 when activating the irrigation module. The distribution of irrigation events throughout the year was also consistent with known irrigation practices in the region. For trees that are drip irrigated, very frequent events every 2 days corresponding to the return time are triggered by the model in summer, while events were sparser in winter

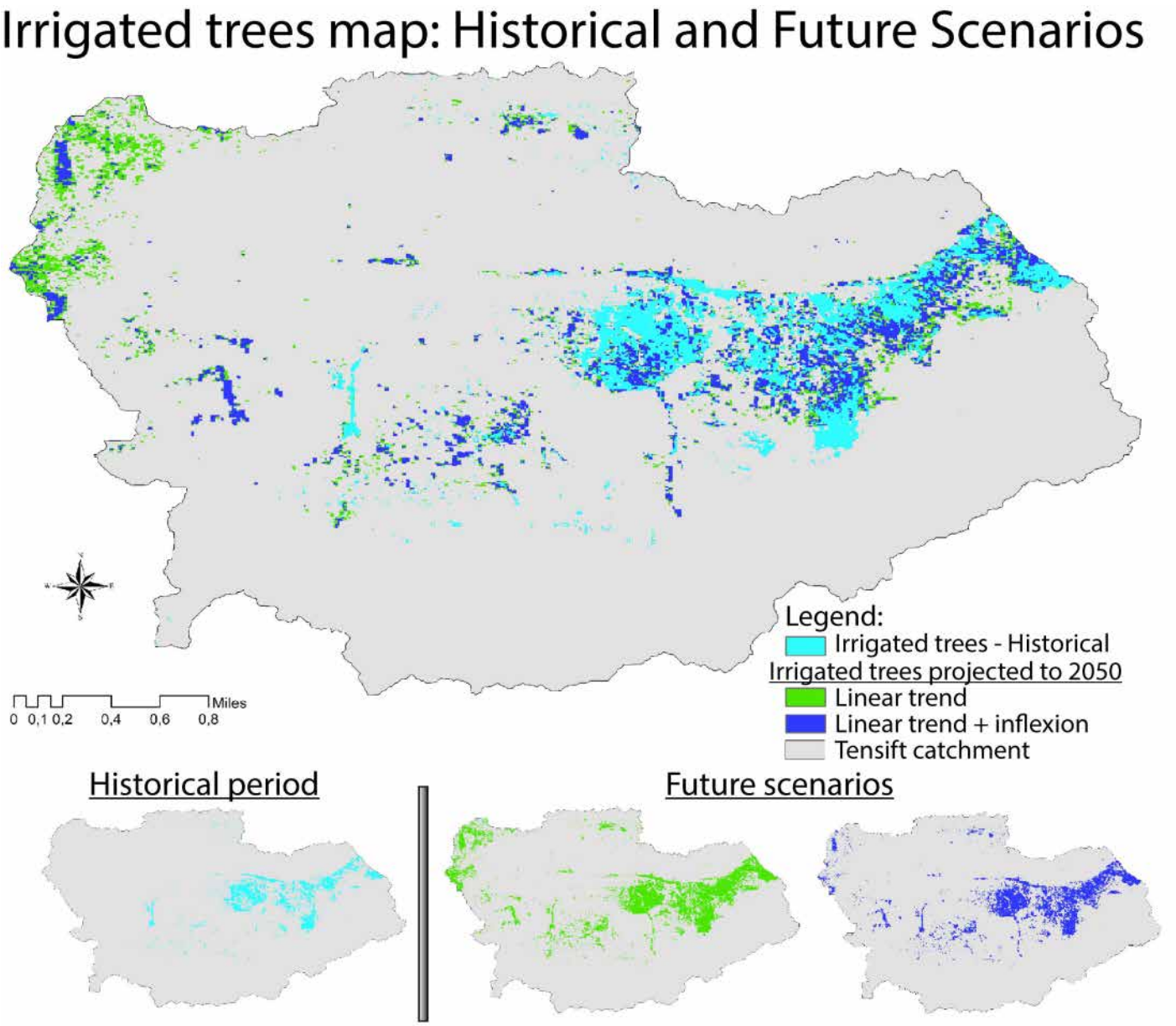

Fig 4. The cover fraction of trees for the historical period to the projected values at the 2050 horizon (see text). All the border shapes are provided by openstreemap (https://www.openstreetmap.org/) under the Open Data Commons (ODbL) licence (https://opendatacommons.org/licenses/odbl/summary/).

https://doi.org/10.1371/journal.pwat.0000297.g004

when the evaporative demand was low and when there was some water supply from rainfall. For wheat, the model predicted 5 to 6 events per season, which was also in agreement with agricultural practices.

Finally, the Bour site was correctly identified as a rainfed field as both experiments perfectly matched. The integration of the new irrigation scheme into the ISBA model has had a positive impact on the model's predictions. The forecasts significantly improved compared to the case where the model did not incorporate irrigation. However, there was a difference between the observations and the simulations with this new scheme. To determine the irrigation water quantity to apply, the model analyzed several variables mentioned in the previous

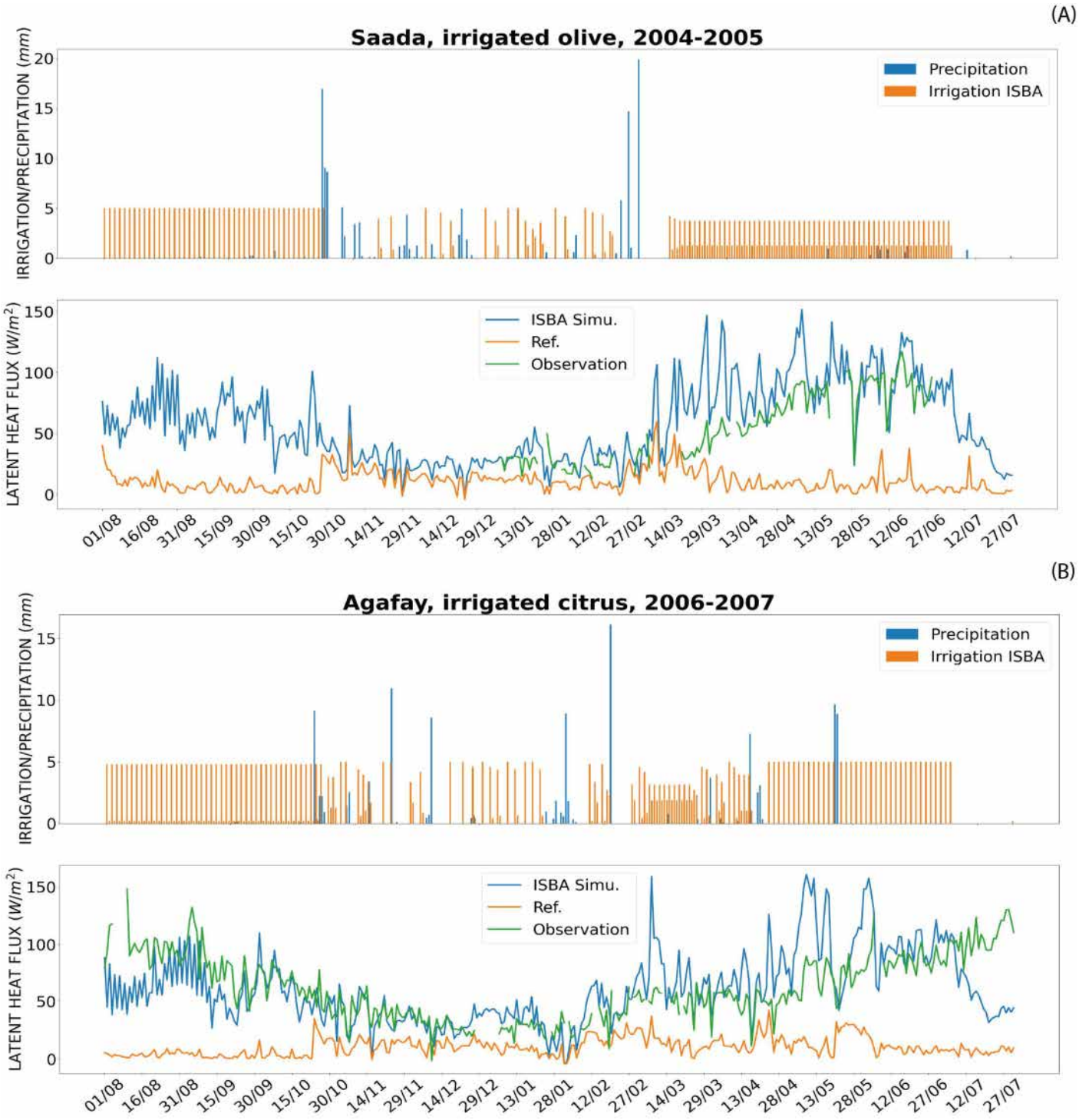

Fig 5. Predictions of latent heat fluxes and irrigation water amounts by the model with and without the irrigation scheme activated for tree crops: subfigure (A) Predictions for olive trees (Saada) - Period 2004/2005, and (B) Predictions for citrus trees (Agafay station) - Period 2006/2007. 'Ref' is for ISBA predictions without irrigation while 'ISBA Simu' stands for ISBA prediction with irrigation.

https://doi.org/10.1371/journal.pwat.0000297.g005

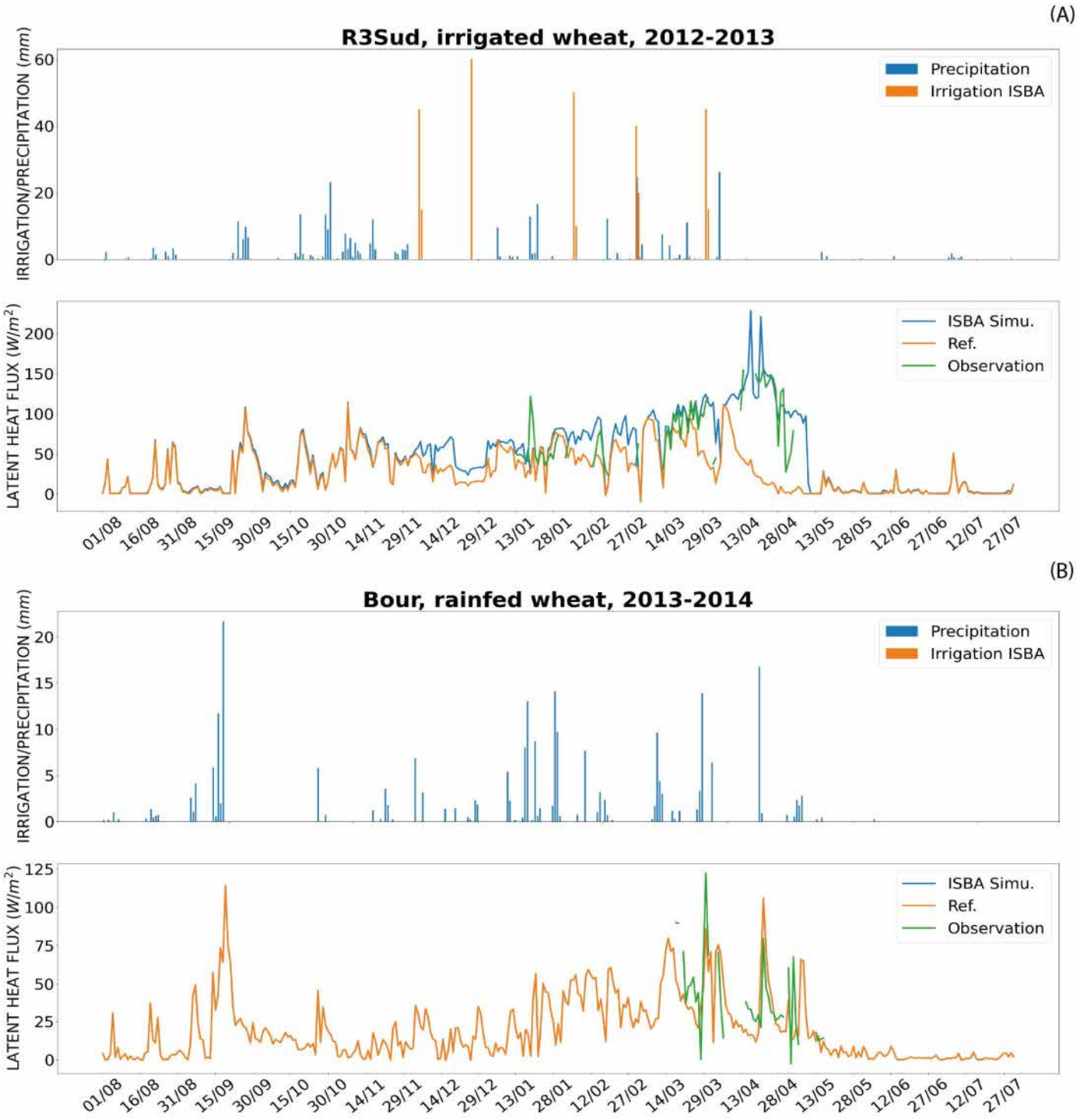

Fig 6. Predictions of latent heat fluxes and irrigation water amounts by the model with and without the irrigation scheme activated for wheat crops, subfigure (A) Predictions for irrigated Wheat (R3_South station) - Period 2012/2013, and (B) Predictions for rainfed Wheat (Bour station) - Period 2013/2014. 'Ref' is for ISBA predictions without irrigation while 'ISBA Simu' stands for ISBA prediction with irrigation.

https://doi.org/10.1371/journal.pwat.0000297.g006

Table 3. Statistical metrics of the comparison between observed and predicted LE on the different sites.

Stations	Year	Observed average	Average predicted (W/m^2)		Bias (W/m^2)		RMSE (W/m^2)		Correlation r	
			EXP1	EXP2	EXP1	EXP2	EXP1	EXP2	EXP1	EXP2
Saada	**2004/2005**	57	11	73	−46	16	55	27	−0.143	0.793
Agdal	**2004/2005**	69	8	46	−60	−22	64	30	−0.047	0.227
Agafay	**2005/2006**	95	13	83	−82	−12	84	36–	0.174	0.184
Saada	**2005/2006**	34	10	39	−24	5	31	20	−0.029	0.561
R3Olivier	**2005/2006**	148	38	90	−110	−58	117	70	0.265	0.415
Agafay	**2006/2007**	62	10	62	−52	0	61	31	−0.216	0.484
R3Olivier	**2006/2007**	154	15	77	−140	−77	149	94	−0.431	0.008
Agafay	**2007/2008**	56	14	52	−42	−4	54	24	−0.305	0.603
R3	**2007/2008**	59	11	98	−48	39	57	54	0.251	0.616
R3Olivier	**2007/2008**	177	5	56	−171	−120	174	124	0.175	0.544
Agafay	**2008/2009**	59	26	60	−32	1	49	31	0.166	0.627
Agafay	**2009/2010**	72	13	57	−60	−15	70	34	−0.130	0.476
R3	**2011/2012**	77	24	68	−52	-9	69	50	0.554	0.573
R3	**2012/2013**	64	28	31	−36	−34	58	56	0.039	0.097
R3Nord	**2012/2013**	60	38	90	−22	30	49	54	−0.059	0.340
R3Sud	**2012/2013**	79	39	86	−40	7	61	29	0.004	0.727
Bour	**2013/2014**	41	34	34	−7	−7	23	23	0.597	0.597

https://doi.org/10.1371/journal.pwat.0000297.t003

section, notably the Soil Water Index (SWI), which was a crucial indicator in the irrigation process. This could partly explain the flow difference (observed and predicted by the model). The model was considered a perfect farmer, contrary to what was done in reality where the choice of irrigation could be linked to customs or traditions which could be far from what should be done in reality.

Irrigation water amounts at the irrigated perimeter scale. Fig 7 displays the comparison of monthly time series of irrigation volume integrated at the scale of the irrigated perimeter provided by ORMVAH and predicted by the model for two irrigated perimeters taken for illustration purpose. The results of the comparison for the other perimeters are displayed in S3 Fig in the supplementary material. The statistical metrics are also reported in Table 4. For all considered perimeters, the predicted water amount was positively biased with respect to the observations.

Water budget of the catchment

This section aims to analyze the seasonal and interannual dynamics of the water budget at the catchment level. To this end, Fig 8 displays the monthly climatology of precipitation, irrigation amounts, evapotranspiration, and drainage in mm/month averaged over the physical catchment area. S4 Fig in the appendix displays the interannual variability of the same four terms of the water budget expressed in millions of cubic meters (Mm^3). Finally, Fig 9 represents the maps of the same yearly average fluxes in mm/month. Supply to the surface/crops is positive (precipitation and irrigation) while losses are negative (evapotranspiration and drainage).

The monthly climatology of precipitation exhibited a clear seasonal cycle with most of the precipitation concentrated between November and May. It was smoother for the whole catchment than for the irrigated areas, which are mostly located in the plain with almost no precipitation in summer, while the catchment includes the mountainous area characterized by a shifted rainfall season with respect to the surrounding plains and storms that can occur

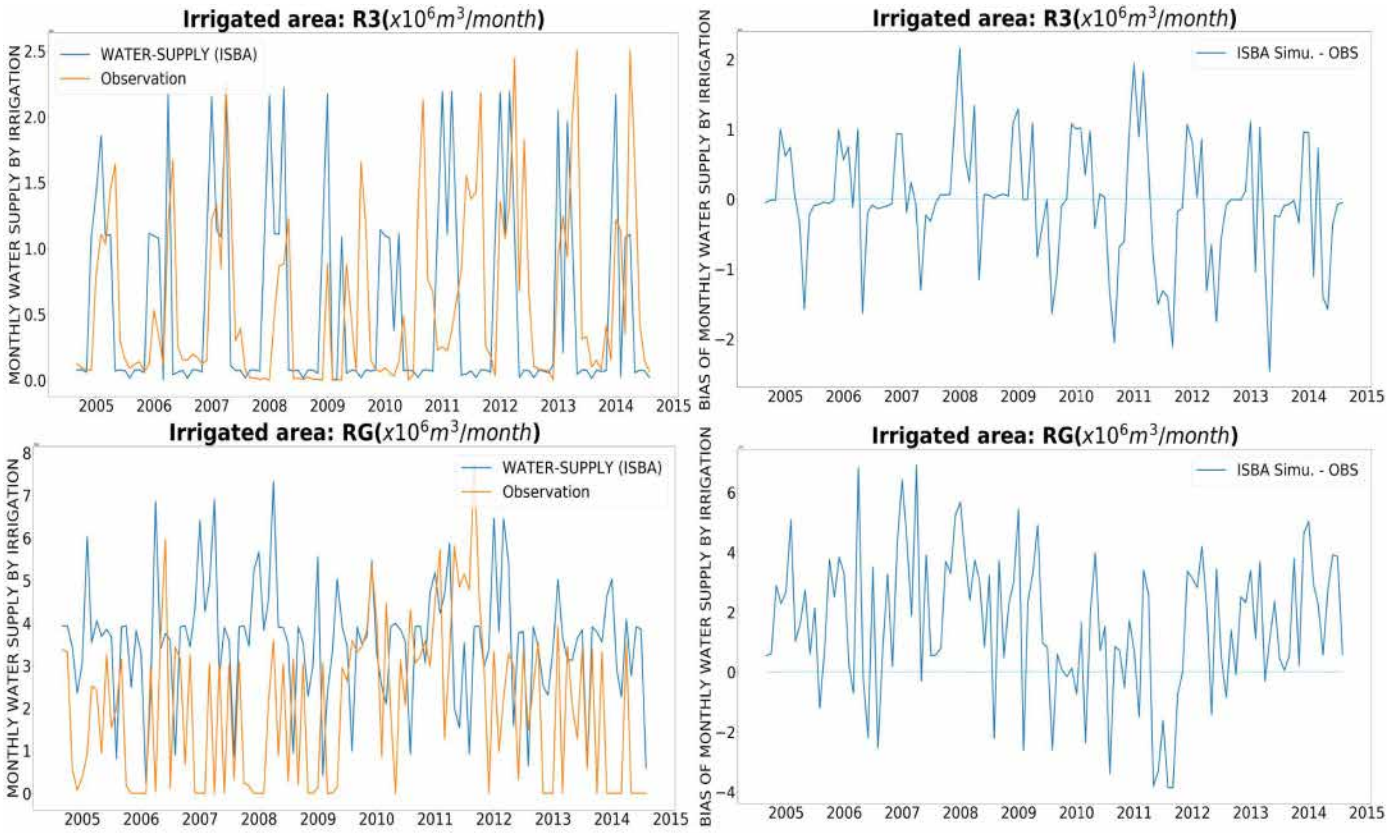

Fig 7. Predictions of monthly irrigation water supplies by the ISBA model with irrigation scheme activated (EXP2) for two irrigated perimeters: R3 (top, left) and RG (bottom, left) for the period 2004/2014, a representation of the difference between the observation and the model prediction was also represented in the Fig for the same perimeters R3 (top, right) and RG (bottom, right).

https://doi.org/10.1371/journal.pwat.0000297.g007

Table 4. Comparison of irrigation water supplies using observations and simulation from the ISBA model with activated irrigation (EXP2), this characterization is carried out using the root mean square error (RMSE), the simple correlation coefficient (R) and bias (Bias). Over the period 2004/2014 for different perimeters.

Irrigated Perimeter	Average Observed	Average predicted $(m^3$ / month$)$	Bias $(m^3$ / month$)$	Bias in %	RMSE $(m^3$ / month$)$	RMSE in %	Simple correlation r
H2	479032	674897	195865	40.9	565554	118	0.074
R1	648272	1019346	371074	57.2	1163567	180	0.293
R3	590803	621683	30880	5.2	936392	159	0.247
Z1	335402	502610	167207	49.8	536298	160	0.188
RG	1991187	3639960	1648773	82.8	3035164	152	-0.052

https://doi.org/10.1371/journal.pwat.0000297.t004

in summer. Irrigation amounts at the scale of the catchment were low as the average amount for the whole region expressed in mm/month was shown. Contrasted seasonal cycles between wheat and trees were observed: irrigation was supplied all year long for trees, with high amounts in summer in response to the high evaporative demand at this time, and lower supplies in winter and early spring during tree dormancy, while wheat was irrigated during the crop cycle in winter and early spring. Irrigation was stopped about one month before harvest in May or early June. On average, over the irrigated areas, about 563mm/year and 1454mm/year were supplied for wheat and tree crops, respectively; this means 5630 and 14540 cubic meter per hectare. Evapotranspiration peaks were observed in late spring for wheat and in

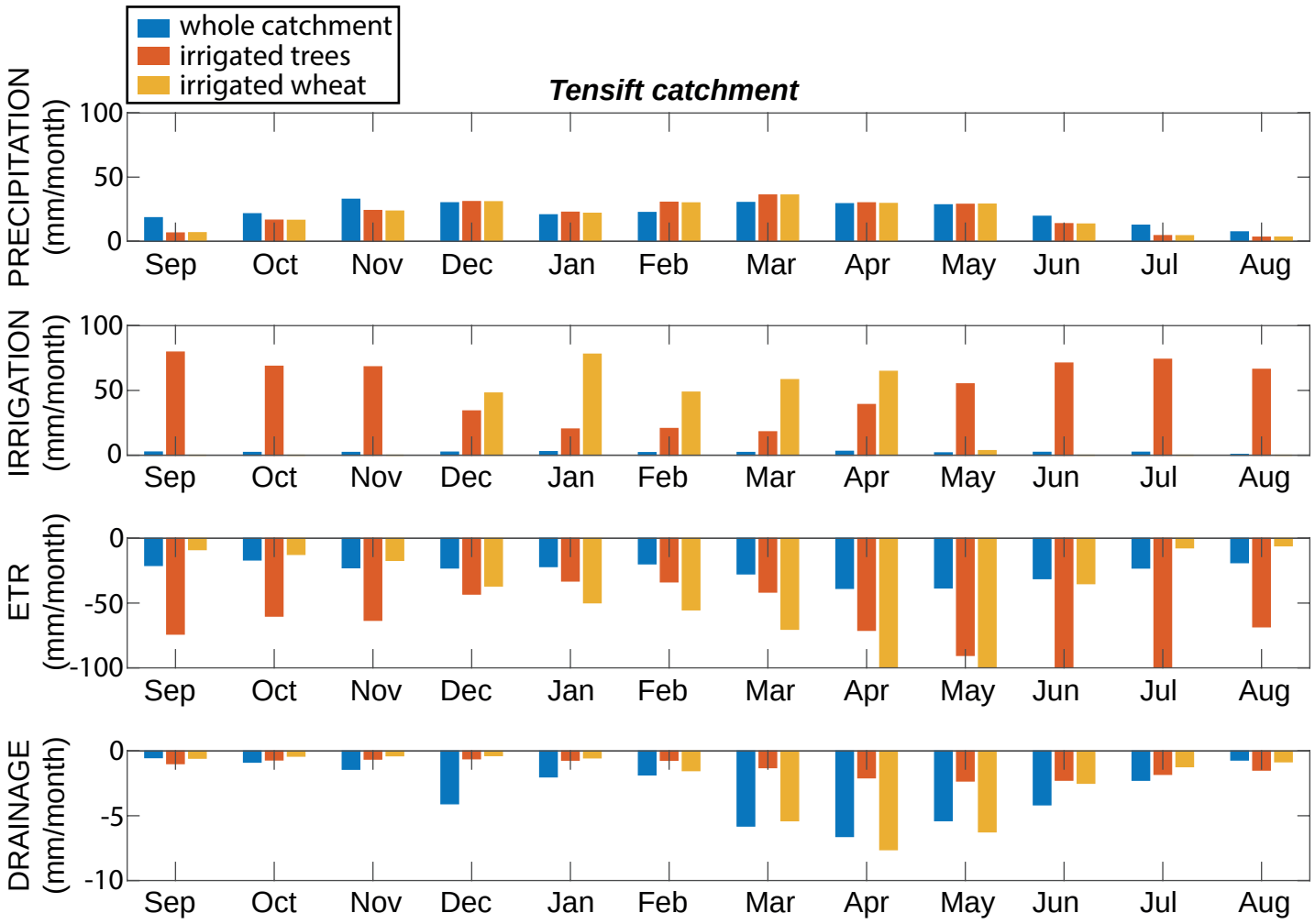

Fig 8. Climatology (2004–2014) of the main terms of the water budget expressed in mm/month including precipitation, irrigation water amounts, evapotranspiration and drainage for the whole catchment, for the irrigated trees areas and for the irrigated wheat areas.

https://doi.org/10.1371/journal.pwat.0000297.g008

summer for trees. Finally, drainage, a key term of the water budget for groundwater resources as it contributes to groundwater table recharge, was an order of magnitude lower than the others three terms. With respect to the catchment average values, drainage fluxes were lower in the irrigated areas, except for wheat in April and May. At this time, wheat starts its senescence stage. In addition, the shallower root system of wheat explained the higher value of drainage fluxes when compared to trees.

Regarding the spatial patterns (Fig 9), rainfalls was concentrated in the higher elevation areas to the south and exhibited a slight west-east gradient, except for the coastal areas to the west. Spatial patterns of evapotranspiration were closely linked to those of rainfall except for the irrigated areas located at the center of the catchment in the plain and, to a lesser extent, on the foothills of the Atlas Mountains, showing the higher evapotranspiration fluxes. The drainage maps supported the previous comment that the drainage fluxes in the irrigated areas were low, as most of the drainage, a strong contribution to the ground water recharge, occurred at the foothills of the Atlas. Finally, S4 Fig in the appendix provides the order of magnitude of the interannual variability of the fluxes and the total water amounts that each represents

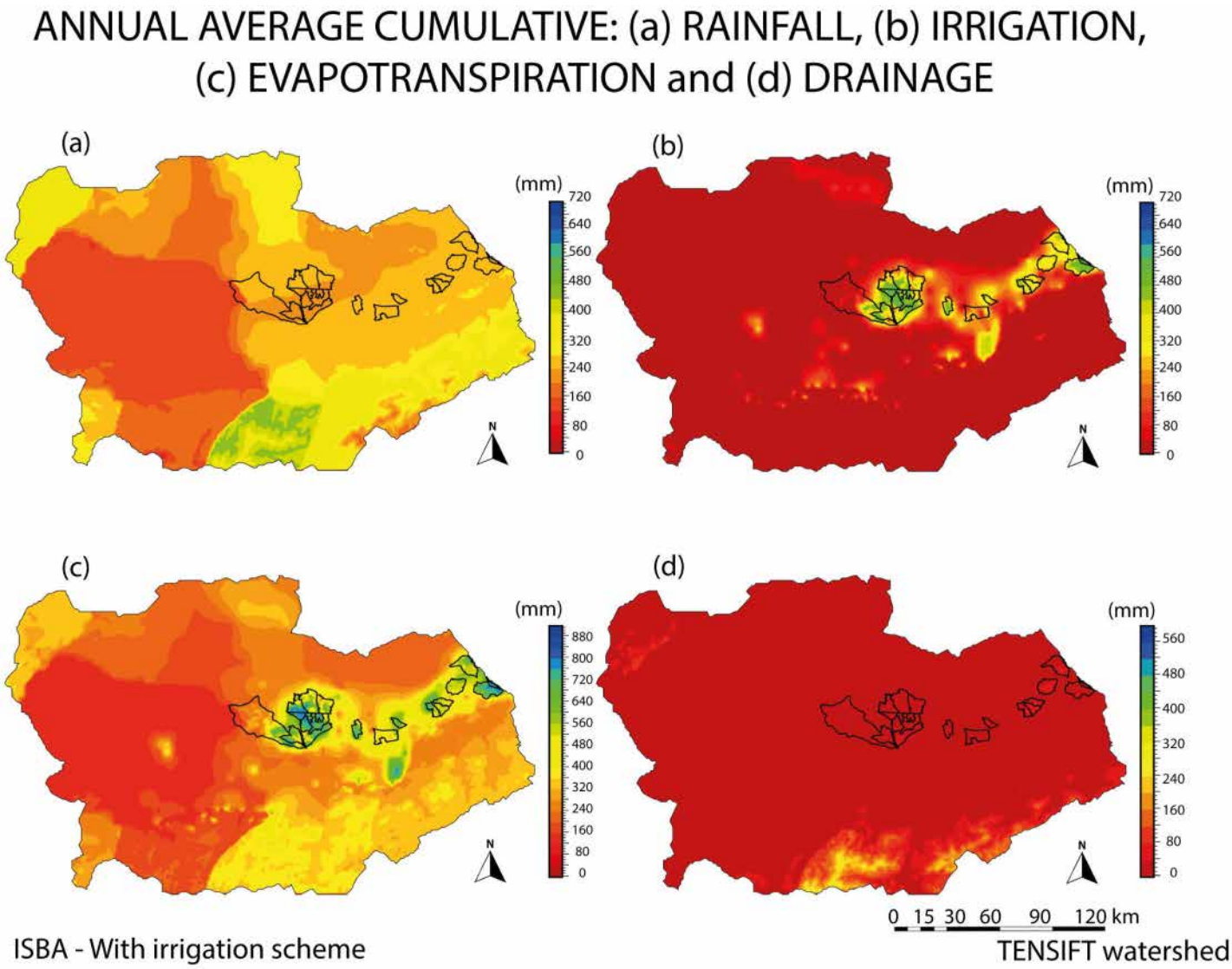

Fig 9. Annual average cumulation over the period 2004–2014 of the parameters: rainfall (a; top left), irrigation (b; top right), evapotranspiration (c; bottom left) and drainage (d; bottom right).

https://doi.org/10.1371/journal.pwat.0000297.g009

at the scale of the catchment in millions of cubic meters ($Mm^3 = 10^6 m^3$). The interannual variability of precipitation amount was strong with a coefficient of variation of 30% (standard deviation divided by the average) and values ranging from 3204 Mm^3 to 7063 Mm^3 for the seasons 2004–2005 and 2008–2009, respectively, which is consistent for these semi-arid areas. Irrigation water supplies ranged from 593 Mm^3 for the season 2008–2009 characterized by heavy rainfall during autumn 2008 and dramatic flooding in the north of the country, to 858 Mm^3 in 2007, one of the two driest years of the study period. Nevertheless, in contrast to rainfall, irrigation amounts were less variable from one year to another (coefficient of variation equal to 12%) meaning that rainfall water supply in the irrigated areas represents a small part of the crop water needs. Evapotranspiration was 5601 Mm^3 on average for the 10-years study period, but this value is probably overestimated as no water routing scheme able to predict streamflow reaching the Atlantic Ocean and leaving the catchment was used in this study.

Nevertheless, most of the river channels were dry riverbeds (ouaadis) with intermittent flow, and water only reached the sea during extreme flooding events. Finally, drainage (494 Mm^3 on average) was the most variable flux from one year to another, with a coefficient of variation of 45%, and was obviously closely related to precipitation supply ($R^2 = 0.58$).

Scenarios of climate and agricultural practice changes

This section aims to analyze the impact of climate change and the conversion to tree crops and expansion of irrigated areas on the main water fluxes of the catchment, including irrigation water supply at the 2050 horizon. To this end, two climate scenarios and two conversion rates of irrigated agriculture to tree crops are considered, and the following 6 experiments are implemented: climate change only for scenarios RCP4.5 and RCP8.5, and 4 other runs combining the two climate scenarios with the baseline scenarios of conversion and a second scenario aiming to mimic an inflection of the linear trend of conversion that could occur in response to an incentive public policy of regulation. For information, the monthly differences of precipitation and temperature between the historical period and both climate change scenarios are plotted at S5 Fig in the appendix.

Fig 10 summarizes the potential changes associated with the scenarios by displaying the yearly fluxes in Mm^3 / year for the whole catchment. As expected, and as already shown by many authors, a decrease of precipitation is expected by the 2050 horizon for both climate change scenarios. At the scale of the catchment, it could represent a drop of 278 Mm^3 / year (-6%) and 1017 Mm^3 / year (-21%) for RCP4.5 and RCP8.5, respectively, compared to the historical period. Nevertheless, as shown in S5 Fig in the appendix, the decrease is not homogeneous throughout the year. Indeed, the bimodal distribution of Moroccan precipitation could be strengthened in the future with a drastic decrease from late autumn to spring reaching

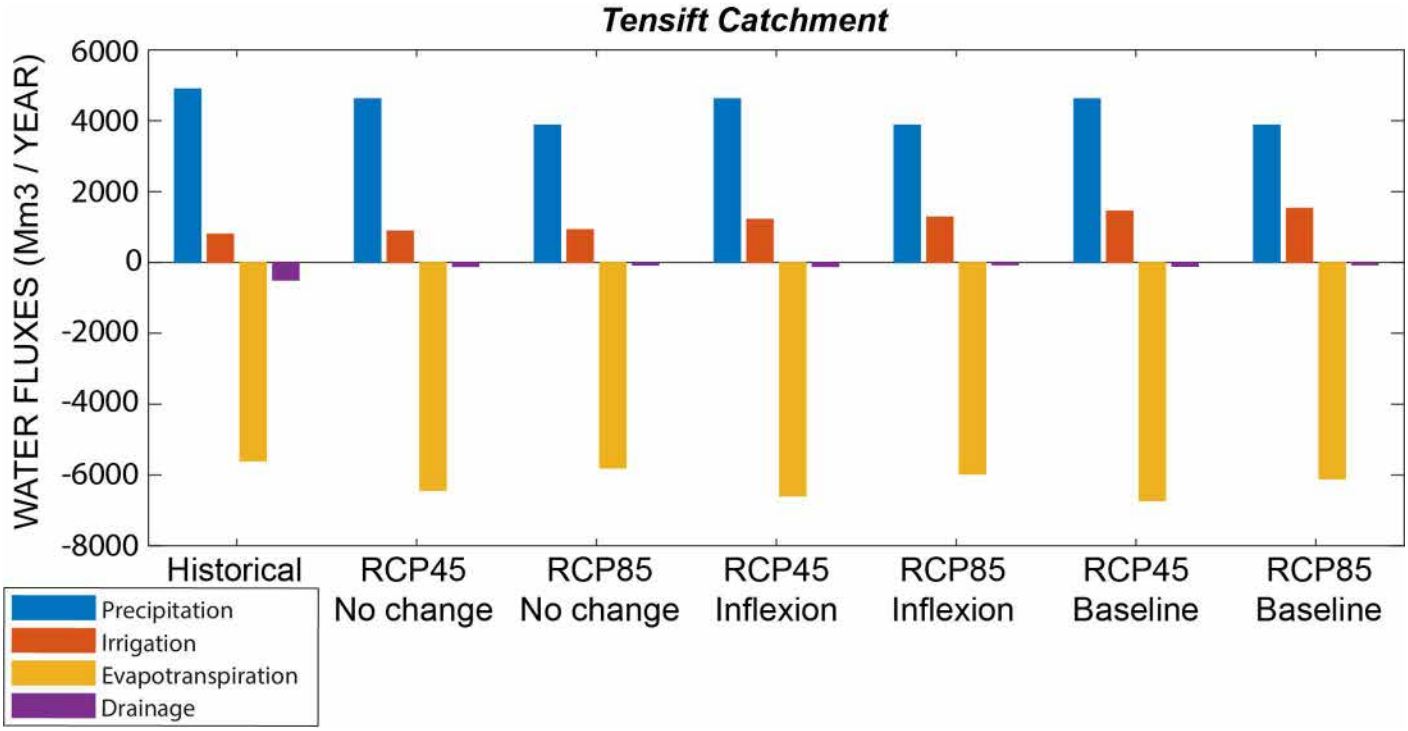

Fig 10. Water fluxes for the historical period and the scenarios: climate scenarios RCP4.5 and RCP8.5 with no change for agriculture and a combination of both climate scenarios with two scenarios of conversion to tree crops and irrigated area expansion (see text).

https://doi.org/10.1371/journal.pwat.0000297.g010

-10mm/month. By contrast, the precipitation loss would be more limited in early autumn, and precipitation could even increase in summer, probably due to more active convection cells above the mountainous areas. Irrigation water supply would be characterized by even stronger changes, as the amount almost doubles for the more extreme scenarios (baseline for agriculture and RCP8.5), going from about 790 Mm^3 for the historical period to more than 1500 Mm^3. The change in irrigation water supply would be mainly impacted by the agricultural scenarios, as when only climate change was considered, the increase of water amount was less than 100 Mm^3 (+10%) and 127 Mm^3 (+16%) for RCP4.5 and RCP8.5, respectively. This increase in irrigation water supply was both related to the drop in precipitation water amount (i.e., more water was needed to meet the plant water needs) and to the temperature rise, which was the highest in spring reaching +3° for RCP8.5 in April and May. Finally, a drastic drop in drainage could occur in response to climate change, going from 494 Mm^3 during the historical period to around 68 Mm^3 for RCP8.5, with close value of 110 Mm^3 for RCP4.5. Change in agriculture did not impact the expected change in the drainage flux. As mentioned earlier, most of the drainage fluxes occur within the Atlas and its foothills, where irrigated agriculture is limited.

To further analyze the data, the historical and future monthly climatologies of the same four fluxes were plotted separately for irrigated trees and irrigated wheat areas at Fig 11 and S6 Fig in the appendix, respectively. Precipitation increases for the scenarios considering changes in the agricultural sector in response to the rise of irrigated tree areas, while, as already shown, a drop is expected for climate change scenarios only (RCP4.5 and RCP8.5 at S5 Fig). Considering irrigation water supply, a marked seasonality was observed for all scenarios, with low values in winter corresponding to the dormancy period of the trees and quite constant and high values during late spring and summer. While warming and precipitation drops associated with climate change hardly impacted irrigation amounts, the intensification of irrigation and extension of irrigated areas almost triple the irrigation water supply for some months. This would occur during the warmest months of the year when precipitation amounts are the lowest. A slight drop in drainage is also observed in response to climate change only, and drainage obviously increased when climate change scenarios were combined with changes in the irrigated areas. Nevertheless, drainage values were two orders of magnitude lower than the other terms of the water budget, meaning that, as mentioned earlier, drainage below the irrigated tree areas is negligible at the scale of the catchment. Thanks to their deep root system, trees are able to take water deeply before it drains below the root zone. By contrast, drainage was an order of magnitude higher for wheat around the crop development peak in March and during early senescence in April, but it was close to zero most of the year (see S6 Fig in the appendix). In addition, drainage dropped for the four scenarios considering both climate and irrigated area changes in response to the conversion of wheat cropped surface into irrigated trees. By contrast with trees, a significant increase in irrigation water amount was observed in December (+25 Mm^3, about +40%) when climate change only was considered. Indeed, at this time, the drop in rainfall was strong and close for both scenarios (see Fig 11 for tree irrigated area and S5 Fig in the appendix for the whole catchment), and wheat was in the development phase with key phenological stages (tillering) requiring water to avoid damage to the crop.

Discussion

A proper representation of agricultural practices in land surface models is essential for both climate studies and the monitoring of water use and resources in strongly anthropized catchments. Within this context, this study aimed (1) to assess the representation of irrigation in the ISBA model embedded in the SURFEX platform by comparison, for the first time, with irrigation data gathered within the Tensift catchment (Morocco); and (2) to analyze potential trajectories of water use under climate change and land use scenarios.

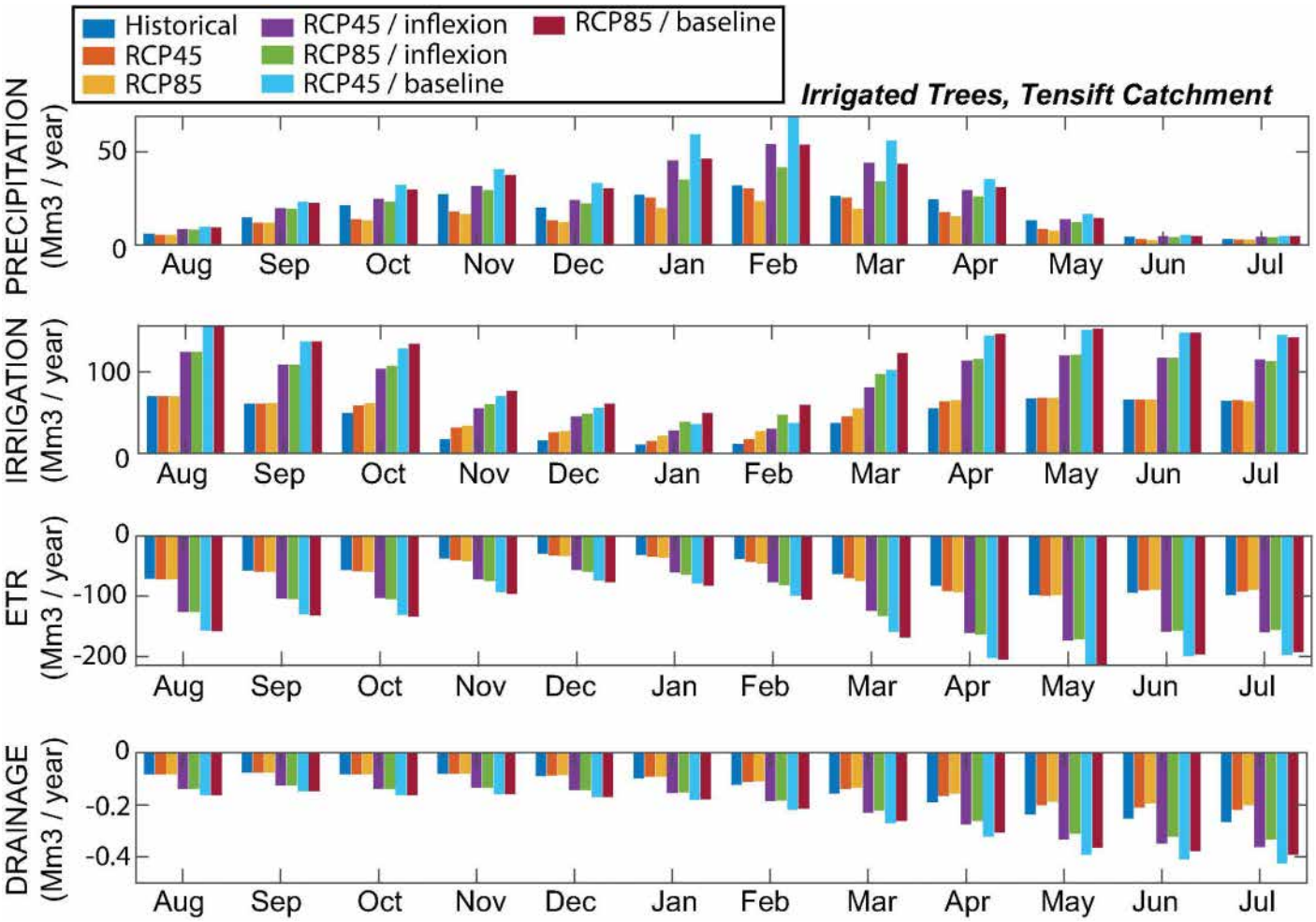

Fig 11. Monthly climatologies of precipitation, irrigation water supply, evapotranspiration and drainage in Mm^3 / *year* cumulated over all the irrigated tree areas for the historical period and the six scenarios.

https://doi.org/10.1371/journal.pwat.0000297.g011

Evaluation of the irrigation scheme

Regarding latent heat fluxes (Fig 5, Fig 6, S1 Fig and S2 Fig), it's important to note that the timing of predicted events may not align with actual water supply dates due to the complexity of irrigation decisions based on farmers' knowledge, economic and environmental factors, and constraints of the irrigation network [76]. This difference may be explained by the fact that the farmer sometimes irrigates more than the plant's needs and sometimes less than what the plant requires, whereas the model assumes a perfect irrigation scenario. Although the irrigation module considerably improved the model predictions of latent heat flux, there were still some scatterings between observations mainly because the meteorological forcing was based on a re-analysis system that is not able to capture the strong variability of rainfall in the region and because the farmer's decision to irrigate may not have been optimal, while the irrigation module of ISBA triggered irrigation every time the soil water index was below a prescribed threshold. In addition, water shortage periods could also limit water availability, constraining farmers to irrigate less than the plant requires.

Irrigation water amounts at the irrigated perimeter scale

Water scarcity and competition between sectors often lead to insufficient water supply by ORMVAH, especially during periods of high demand: drinking water is given priority with respect to irrigation, and tree crops are prioritized with respect to annuals such as wheat. The situation is worsening by the year, and no water at all was attributed to this irrigation sector for the last two crop seasons in 2022 and 2023.

This led to the digging of many boreholes since the early 2000s that were used to complement the surface water provided by ORMVAH ([19,77]. Most of these boreholes were not counted. The R3 area (Fig 7) was characterized by the dominance of wheat [52] as illustrated by the strong seasonality of the monthly water amounts with irrigation supplies being concentrated during the winter months with almost no water provided in summer (perimeters Z1 and R1 exhibited similar behaviour, cf. S3 Fig in the supplementary material). This was properly reproduced by the model which was also able to simulate the two peaks of irrigation in autumn and early spring and the drop of irrigation amounts in January, but with a slight time shift at the start of the season that could be attributed to the choice of the seeding date which was likely a little too early. Likewise, the model tended to stop irrigation earlier than what was "observed" meaning also that harvest occurred about two weeks later than prescribed in the irrigation module. As already mentioned, the interannual variability of supplied water was difficult to analyze because it was related to the filling rate of the surrounding dams at the start of the season and also to the water consumption of the previous seasons. Nevertheless, autumn and winter 2008 faced important rainfall leading to strong damage in the north of the country. This was well depicted by the lower water amount supplied by ORMVAH during the winter crop season 2008–2009 and, to a lesser extent, by the predicted amount by the model. Interestingly enough, the seasonality of supplied water for 2009–2010 and 2010–2011 strongly contrasted with the rest of the time series due to the large quantities provided during summer. Indeed, at this time, industrial groups fostered beet cultivation by providing farmers with agricultural inputs and advice. The beet was seeded in spring and harvested in autumn, explaining the large water amount supplied in summer. This couldn't obviously be reproduced by the model, showing the limit of a static land cover map when agricultural practices change suddenly, such as at this time. Perimeters Z1 and, by contrast, the RG irrigated perimeter located west of Marrakech (Fig 2) were largely composed of tree crops, mainly Olive, with water supplied all year long. Although the order of magnitude was fine, the discrepancies between model and observations were stronger than for R3. Indeed, as for the other perimeters, water shortage and competition may have limited the available water for irrigation as already highlighted, but the irrigation practices for trees were also more complex than for annuals. In particular, late autumn is the period of Olive harvest that is followed in early winter by tree cutting; irrigation supply was very low at this time and these specific practices are not represented in the model. As a conclusion, a perfect match between predicted and observed water supply was not expected because of specific practices and limited water availability that precluded ORMVAH from providing water to farmers corresponding to the plant water needs, but the order of magnitude and the seasonality of supply for wheat and, to a lesser extent, for tree crops was correctly reproduced by the model.

To summarize, significant mismatch between predicted irrigation amounts based on the estimated crop water need and "observed" irrigation were expected in particular on short time scales. Indeed, irrigation decisions were partly governed by the farmer's experience and local specificities such as the need for soil leaching to reduce salinity [78], which usually leads to over-irrigation with respect to the plant's water needs. Farmers' decisions were also often based on thier own knowledge and beliefs and could be far from the optimal needs

of the crops, as shown by [79], whose results demonstrated that these empirical decisions could lead to significant loss of water through deep percolation for drip-equipped fields or by soil evaporation for flooding techniques. Likewise, Benouniche et al. [80] in the Saiss region (Morocco) showed that, also because of a lack of know-how on this new irrigation technique of the irrigators, over-irrigation on drip-equipped fields that could range from 25% to 90% was a common practice in this region. In addition, the office in charge of managing irrigation distribution to equipped irrigated perimeters was often constrained by water availability. Indeed, water amounts were allocated to agriculture once the drinking water sector was satisfied, meaning that crop water needs were not considered in case of water shortage. As these water scarcity situations were expected to increase in the future [2], water supplied to the crops would be even further from the real water needs. Unfortunately, in situ irrigation data that could help to improve irrigation parameterization into land surface model are very scarce [81], but recent research on the retrieval of irrigation timing and amount from satellite data is promising [82–85] and will certainly contribute to a better accounting of irrigation practices in the future. Despite the rough representation of irrigation decision rules in land surface models, the results of this study demonstrated that predicted irrigation estimates with a reasonable accuracy could be expected on longer time scales from monthly to seasonal.

Water budget of the catchment

Another striking point was the relatively low amounts of deep drainage on the plain irrigated areas (see Fig 9), apart from the spring months for wheat, while drainage was a key process of groundwater recharge. In semi-arid areas, the recharge processes of the plain water table typically consisted of precipitation infiltration, water return from irrigation, subsurface inflows originating from the upper areas (called mountain block recharge; [86], and runoff water mainly during flood events. The last two items were called mountainous front recharge [87], and it was generally accepted that they were the dominating processes on semi-arid catchments [88]. Our results showing low water return to the water table below the irrigated areas on the plain were in overall agreement with the findings of [89], who demonstrated that aquifer recharge in the study region was dominated by diffuse recharge of rainwater and along the river beds through runoff, partly originating from snowmelt [44,90]. Bouimouass et al. [91] also highlighted that water return from irrigation could be high, even exceeding the natural recharge processes through runoff and precipitation infiltration, but only for the foothills areas where water was diverted from the riverbeds, in agreement with the pattern of high drainage values to the south of the catchment in Fig 9. This means that, in terms of recharge flow, the extension and intensification of irrigated areas that occurred mainly in the plain [19] would not compensate the expected decrease in river flows in response to climate change [92], thus strengthening the unsustainable use of groundwater in the region.

Drip irrigation has been largely promoted in Morocco with the initial objective to save water since the green plan for Moroccan agriculture in 2008, with subsidies that can reach 100%. It was also largely accepted by irrigators as it reduced labor costs and increased income and yields [93]. This drastic change in irrigation practices has been associated with the conversion to more water-intensive crops, as shown by the time series of satellite land use maps [19], the surge in the number of private drillings outside any legal framework [94], and consequently, a strong increase in agricultural water use since early 2010 [95]. This rebound effect of switching to drip irrigation has been the subject of a large body of literature and has already been observed worldwide [96].

Analyzing potential trajectories of water use under climate change and land use scenarios

The results of the future scenarios demonstrated that this rebound effect would impact agricultural water use more drastically than the rise in evaporative demand due to warming. For the baseline scenario, irrigation amounts could even double by the 2050 horizon (about 1528 Mm3/year for the RCP8.5 scenario), thus exerting unsustainable pressure on aquifers facing a drastic drop in recharge due to a decrease in rainfall inputs, but also due to the conversion to tree crops capable of extracting water deeper in the soil than annuals. Within this context, one of the major weaknesses of this study was that it did not establish the link between agricultural consumption and available water in surface and groundwater reservoirs to analyze the sustainability of irrigated agriculture in the region. Indeed, some studies have already pointed out that, under a baseline scenario, some regions could be dewatered as early as 2030 [11]. Another limit that should also be the object of research is the consideration of the effects of rising temperatures and atmospheric CO2 on plant phenology and physiology. Indeed, increased atmospheric CO2 may improve stomatal closure processes and regulate plant transpiration [97,98], while rising temperatures could reduce the length of the growing season for cereals [99], but also increase heat stress periods that could negatively impact plant production. This could in turn affect the seasonal irrigation patterns of cereals as shown by [4].

This conversion to water-intensive trees has also drastically changed the seasonal patterns of irrigation water requirements, with a peak of demand concomitant with the hottest and driest months of the year when surface and groundwater reservoirs were highly exploited, and water needs throughout the year, while cereal consumption has extended into the winter and spring months. This adds severe constraints to the management system and could make the region much more vulnerable to droughts. Indeed, while surface water supply to cereals could be stopped to maintain tree crops alive in cases of water shortage when the area cropped with trees was low, the available water would not even be sufficient to irrigate trees if the cropped area increased. The perverse effect of this situation could indirectly encourage farmers to dig new wells to ensure their water self-sufficiency.

Summary and conclusion

This study provided a comprehensive evaluation of a new irrigation scheme capable of operating on a global scale, implemented within the ISBA land surface model to enhance the representation of agricultural water use, focusing on the predictions of latent heat flux and irrigation amounts in the semi-arid Tensift watershed. The results demonstrated the module's effectiveness in improving model performance, reducing biases, and enhancing the representation of dynamic processes, especially during periods of high evaporation demand. The assessment of irrigation amounts at the scale of the irrigated perimeter revealed the model's ability to capture the temporal distribution of irrigation events. Despite a positive bias in the predicted water amounts, the model successfully reproduced the general order of magnitude and the seasonality. Exploration of future scenarios, including climate change and changes in agricultural practices, revealed that irrigation water use could almost double for the more extreme scenarios and that most of this drastic increase is attributed to land use change, including irrigation intensification and expansion. These results also demonstrate that seasonal water supply patterns could be significantly altered, with peaks coinciding with the hottest and driest months of the year, thereby heavily constraining the water resource management system in the region.

In conclusion, this study offers valuable insights into water resource dynamics in semi-arid regions, aiding informed decision-making for sustainable water management, crop selection,

and the promotion of efficient agricultural practices. It also evaluates public policies that support the transition to drip irrigation. Additionally, the study paves the way for assessing future water resource trajectories, including surface and groundwater reservoirs, while considering agricultural practices.

Supporting information

S1 Fig. Predictions of latent heat fluxes and irrigation water amounts by the model with and without the irrigation scheme activated for trees and wheat crops, for different stations and all-time series.
(TIFF)

S2 Fig. Predictions of sensible heat fluxes and irrigation water amounts by the model with and without the irrigation scheme activated for trees and wheat crops, for different stations and all-time series.
(TIFF)

S3 Fig. Predictions of monthly irrigation water supplies by the ISBA model with irrigation scheme activated at left side of figure, for the period 2004/2014. A representation of the difference between the observation and the model prediction was also represented in the figure for the same perimeters at the right side, for different irrigation perimeters.
(TIFF)

S4 Fig. Interannual variability of precipitation, irrigation supplies, evapotranspiration and drainage expressed in millions of cubic meters on the Tensift catchment.
(TIFF)

S5 Fig. Monthly differences of air temperature (left) and precipitation (right) between the historical period and both RCP45 and RCP85 climate change scenarios at the scale of the whole Tensift catchment for the 2050s horizon.
(TIFF)

S6 Fig. Monthly climatologies of precipitation, irrigation water supply, evapotranspiration and drainage in M m3/ year cumulated over all the irrigated tree areas for the historical period and the six scenarios.
(TIFF)

S7 Fig. Annual cumulative irrigation map estimated by the ISBA model, using the new irrigation scheme, for the period 2004–2014. at the Tensift watershed. All the border shapes are provided by openstreemap (https://www.openstreetmap.org/) under the Open Data Commons (ODbL) licence (https://opendatacommons.org/licenses/odbl/summary/).
(TIFF)

S8 Fig. Annual cumulative evapotranspiration map estimated by the ISBA model, using the new irrigation scheme, for the period 2004–2014. at the level of the Tensift catchment area. All the border shapes are provided by openstreemap (https://www.openstreetmap.org/) under the Open Data Commons (ODbL) licence (https://opendatacommons.org/licenses/odbl/summary/).
(TIFF)

S9 Fig. Annual cumulative rainfall map estimated by SAFRAN model using by the ISBA model, for the period 2004–2014. at the level of the Tensift catchment area. All the border shapes are provided by openstreemap (https://www.openstreetmap.org/) under

the Open Data Commons (ODbL) licence (https://opendatacommons.org/licenses/odbl/summary/).
(TIFF)

S10 Fig. Annual cumulative drainage map estimated by the ISBA model, using the new irrigation scheme, for the period 2004–2014. at the Tensift watershed. All the border shapes are provided by openstreemap (https://www.openstreetmap.org/) under the Open Data Commons (ODbL) licence (https://opendatacommons.org/licenses/odbl/summary/).
(TIFF)

Author contributions

Conceptualization: Lionel Jarlan, Lahoucine Hanich.

Formal analysis: Ahmed Moucha.

Funding acquisition: Lionel Jarlan, Lahoucine Hanich.

Investigation: Ahmed Moucha, Lionel Jarlan, Pere Quintana-Segui, Anais Barella-Ortiz, Michel Le Page, Lahoucine Hanich.

Methodology: Lionel Jarlan, Pere Quintana-Segui, Simon Munier, Lahoucine Hanich.

Resources: Michel Le Page, Simon Munier, Adnane Chakir, Aaron Boone, Fatallah Sghrer, Jean-Christophe Calvet.

Supervision: Lionel Jarlan, Pere Quintana-Segui, Anais Barella-Ortiz, Simon Munier, Aaron Boone, Jean-Christophe Calvet, Lahoucine Hanich.

Visualization: Ahmed Moucha.

Writing – original draft: Ahmed Moucha, Lionel Jarlan, Lahoucine Hanich.

Writing – review & editing: Pere Quintana-Segui, Anais Barella-Ortiz, Michel Le Page, Simon Munier, Adnane Chakir, Aaron Boone, Fatallah Sghrer, Jean-Christophe Calvet.

Références

1. Lionello P, Abrantes F, Gacic M, Planton S, Trigo R, Ulbrich U. The climate of the Mediterranean region: research progress and climate change impacts. Reg Environ Change. 2014;14(5):1679–84. https://doi.org/10.1007/s10113-014-0666-0
2. Tramblay Y, Koutroulis A, Samaniego L, Vicente-Serrano SM, Volaire F, Boone A, et al. Challenges for drought assessment in the mediterranean region under future climate scenarios. Earth Sci Rev. 2020;210:103348. https://doi.org/10.1016/j.earscirev.2020.103348
3. FAO-AQUASTAT. Food and Agriculture Organization of the United Nations (FAO). 2016. [Cited 2023 Oct 24]. http://www.fao.org/nr/water/aquastat/data/query/index.html?lang=en
4. Bouras E, Jarlan L, Khabba S, Er-Raki S, Dezetter A, Sghir F, et al. Assessing the impact of global climate changes on irrigated wheat yields and water requirements in a semi-arid environment of Morocco. Sci Rep. 2019;9(1):19142. https://doi.org/10.1038/s41598-019-55251-2 PMID: 31844076
5. Tramblay Y, Jarlan L, Hanich L, Somot S. Future scenarios of surface water resources availability in north african dams. Water Resour Manage. 2017;32(4):1291–306. https://doi.org/10.1007/s11269-017-1870-8
6. Schilling J, Freier KP, Hertig E, Scheffran J. Climate change, vulnerability and adaptation in North Africa with focus on Morocco. Agric Ecosyst Environ. 2012;156:12–26.
7. Schilling J, Hertig E, Tramblay Y, Scheffran J. Climate change vulnerability, water resources and social implications in North Africa. Reg Environ Change. 2020;20(1). https://doi.org/10.1007/s10113-020-01597-7
8. Wada Y, van Beek LPH, van Kempen CM, Reckman JWTM, Vasak S, Bierkens MFP. Global depletion of groundwater resources. Geophys Res Lett. 2010;37(20):. https://doi.org/10.1029/2010gl044571
9. Famiglietti JS. The global groundwater crisis. Nat Clim Chang. 2014;4:945–8.

10. Scanlon BR, Fakhreddine S, Rateb A, de Graaf I, Famiglietti J, Gleeson T, et al. Global water resources and the role of groundwater in a resilient water future. Nat Rev Earth Environ. 2023;4(2):87–101. https://doi.org/10.1038/s43017-022-00378-6
11. Le Page M, Berjamy B, Fakir Y, Bourgin F, Jarlan L, Abourida A, et al. An Integrated DSS for groundwater management based on remote sensing. the case of a semi-arid aquifer in Morocco. Water Resour Manage. 2012;26(11):3209–30. https://doi.org/10.1007/s11269-012-0068-3
12. Jarlan L, Khabba S, Er-Raki S, Le Page M, Hanich L, Fakir Y. Remote sensing of water resources in semi-arid Mediterranean areas: the joint international laboratory TREMA. Int J Remote Sens. 2015;36:4879–917.
13. Wisser D, Frolking S, Douglas EM, Fekete BM, Vörösmarty CJ, Schumann AH. Global irrigation water demand: variability and uncertainties arising from agricultural and climate data sets. Geophys Res Lett. 2008;35(24). https://doi.org/10.1029/2008gl035296
14. Puy A, Sheikholeslami R, Gupta HV, Hall JW, Lankford B, Lo Piano S, et al. The delusive accuracy of global irrigation water withdrawal estimates. Nat Commun. 2022;13(1):3183. https://doi.org/10.1038/s41467-022-30731-8 PMID: 35676249
15. Saadi S, Todorovic M, Tanasijevic L, Pereira LS, Pizzigalli C, Lionello P. Climate change and Mediterranean agriculture: impacts on winter wheat and tomato crop evapotranspiration, irrigation requirements and yield. Agric Water Manag. 2015;147:103–15. https://doi.org/10.1016/j.agwat.2014.05.008
16. Wada Y, Wisser D, Eisner S, Flörke M, Gerten D, Haddeland I. Multimodel projections and uncertainties of irrigation water demand under climate change. Geophys Res Lett. 2013;40:4626–32.
17. Lovelli S, Perniola M, Di Tommaso T, Ventrella D, Moriondo M, Amato M. Effects of rising atmospheric CO2 on crop evapotranspiration in a mediterranean area. Agric Water Manag. 2010;97(9):1287–92. https://doi.org/10.1016/j.agwat.2010.03.005
18. Gorguner M, Kavvas ML. Modeling impacts of future climate change on reservoir storages and irrigation water demands in a mediterranean basin. Sci Total Environ. 2020;748:141246. https://doi.org/10.1016/j.scitotenv.2020.141246 PMID: 32798863
19. Ouassanouan Y, Fakir Y, Simonneaux V, Kharrou MH, Bouimouass H, Najar I, et al. Multi-decadal analysis of water resources and agricultural change in a Mediterranean semiarid irrigated piedmont under water scarcity and human interaction. Sci Total Environ. 2022;834:155328. https://doi.org/10.1016/j.scitotenv.2022.155328 PMID: 35452720
20. Le Page M, Fakir Y, Jarlan L, Boone A, Berjamy B, Khabba S, et al. Projection of irrigation water demand based on the simulation of synthetic crop coefficients and climate change. Hydrol Earth Syst Sci. 2021;25(2):637–51. https://doi.org/10.5194/hess-25-637-2021
21. Valverde P, Serralheiro R, de Carvalho M, Maia R, Oliveira B, Ramos V. Climate change impacts on irrigated agriculture in the Guadiana river basin (Portugal). Agric Water Manag. 2015;152:17–30. https://doi.org/10.1016/j.agwat.2014.12.012
22. Rodríguez Díaz JA, Weatherhead EK, Knox JW, Camacho E. Climate change impacts on irrigation water requirements in the Guadalquivir river basin in Spain. Reg Environ Change. 2007;7(3):149–59. https://doi.org/10.1007/s10113-007-0035-3
23. Fader M, Shi S, von Bloh W, Bondeau A, Cramer W. Mediterranean irrigation under climate change: more efficient irrigation needed to compensate for increases in irrigation water requirements. Hydrol Earth Syst Sci. 2016;20(2):953–73. https://doi.org/10.5194/hess-20-953-2016
24. Lawston P, Santanello J, Zaitchik B, Rodell M. Impact of irrigation methods on land surface model spinup and initialization of WRF forecasts. J Hydrometeorol. 2015;16:1135–54.
25. Ozdogan M, Rodell M, Beaudoing HK, Toll DL. Simulating the effects of irrigation over the United States in a land surface model based on satellite-derived agricultural data. J Hydrometeorol. 2010;11:171–84.
26. Chen Y, Niu J, Kang S, Zhang X. Effects of irrigation on water and energy balances in the Heihe River basin using VIC model under different irrigation scenarios. Sci Total Environ. 2018;645:1183–93. https://doi.org/10.1016/j.scitotenv.2018.07.254 PMID: 30248843
27. Lei H, Yang D. Interannual and seasonal variability in evapotranspiration and energy partitioning over an irrigated cropland in the North China Plain. Agric For Meteorol. 2010;150:581–9.
28. Hartmann DL. Global physical climatology: Second edition. 2015.
29. DeAngelis A, Dominguez F, Fan Y, Robock A, Kustu MD, Robinson D. Evidence of enhanced precipitation due to irrigation over the Great Plains of the United States. J Geophys Res. 2010;115(D15). https://doi.org/10.1029/2010jd013892

30. Boone A, Bellvert J, Best M, Brooke J, Canut-Rocafort G, Cuxart J. Updates on the International Land Surface Interactions with the Atmosphere over the Iberian Semi-Arid Environment (LIAISE) Field Campaign. 2021.

31. Zaitchik B, Evans J, Smith R. MODIS-derived boundary conditions for a mesoscale climate model: application to irrigated agriculture in the Euphrates basin. 2005.

32. Wada Y, Bierkens MFP, de Roo A, Dirmeyer PA, Famiglietti JS, Hanasaki N, et al. Human–water interface in hydrological modelling: current status and future directions. Hydrol Earth Syst Sci. 2017;21(8):4169–93. https://doi.org/10.5194/hess-21-4169-2017

33. Zohaib M, Umair M, Choi M. Improving land-surface model simulations in irrigated areas by incorporating soil moisture–based irrigation estimates in community land model. J Irrig Drain Eng. 2022;148(11). https://doi.org/10.1061/(asce)ir.1943-4774.0001716

34. Albergel C, Munier S, Bocher A, Bonan B, Zheng Y, Draper C, et al. LDAS-Monde sequential assimilation of satellite derived observations applied to the contiguous US: An ERA-5 driven reanalysis of the land surface variables. Remote Sensing. 2018;10(10):1627. https://doi.org/10.3390/rs10101627

35. Voirin-Morel S. Modélisation distribuée des flux d'eau et d'énergie et des débits à l'échelle régionale du bassin Adour-Garonne. 2003.

36. Calvet J-C, Gibelin A-L, Roujean J-L, Martin E, Le Moigne P, Douville H. Atmospheric chemistry and physics past and future scenarios of the effect of carbon dioxide on plant growth and transpiration for three vegetation types of southwestern France. Atmos Chem Phys. 2008.

37. McDermid SS, Mearns LO, Ruane AC. Representing agriculture in Earth System Models: approaches and priorities for development. J Adv Model Earth Syst. 2017;9(5):2230–65. https://doi.org/10.1002/2016MS000749 PMID: 30574266

38. Zhou X, Polcher J, Dumas P. Representing human water management in a land surface model using a supply/demand approach. Water Resour Res. 2021;57(4). https://doi.org/10.1029/2020wr028133

39. Xia Q, Liu P, Fan Y, Cheng L, An R, Xie K, et al. Representing irrigation processes in the land surface-hydrological model and a case study in the Yangtze river Basin, China. J Adv Model Earth Syst. 2022;14(7). https://doi.org/10.1029/2021ms002653

40. Martens B, Miralles DG, Lievens H, Van Der Schalie R, De Jeu RAM, Fernández-Prieto D, et al. GLEAM v3: satellite-based land evaporation and root-zone soil moisture. Geosci Model Dev. 2017;10:1903–25.

41. Druel A, Munier S, Mucia A, Albergel C, Calvet J. Implementation of a new crop phenology and irrigation scheme in the ISBA land surface model using SURFEX-v8.1. Geosci Model Dev. 2022;15:8453–71.

42. Foster T, Mieno T, Brozović N. Satellite-based monitoring of irrigation water use: assessing measurement errors and their implications for agricultural water management policy. Water Resour Res. 2020;56(11). https://doi.org/10.1029/2020wr028378

43. Chehbouni A, Escadafal R, Duchemin B, Boulet G, Simonneaux V, Dedieu G. An integrated modelling and remote sensing approach for hydrological study in arid and semi-arid regions: The SUDMED programme. Int J Remote Sens. 2008;29:5161–81.

44. Hanich L, Chehbouni A, Gascoin S, Boudhar A, Jarlan L, Tramblay Y, et al. Snow hydrology in the Moroccan Atlas Mountains. J Hydrol: Reg Stud. 2022;42:101101. https://doi.org/10.1016/j.ejrh.2022.101101

45. Quintana-Segui P, Lemoigne P, Durand Y, Martin E, Habets F, Baillon M. Analysis of near surface atmospheric variables: validation of the SAFRAN analysis over France. J App Meteorol Climatol. 2008;47:92–107.

46. Jacob D, Petersen J, Eggert B, Alias A, Bøssing Christensen O, Bouwer L. EURO-CORDEX: new high-resolution climate change projections for european impact research. Reg Environ Change. 2014;14:563–78.

47. Déqué M. Frequency of precipitation and temperature extremes over France in an anthropogenic scenario: model results and statistical correction according to observed values. Glob Planet Change. 2007;57:16–26.

48. Maraun D, Wetterhall F, Ireson AM, Chandler RE, Kendon EJ, Widmann M, et al. Precipitation downscaling under climate change: Recent developments to bridge the gap between dynamical models and the end user. Rev Geophys. 2010;48(3). https://doi.org/10.1029/2009rg000314

49. Moucha A, Hanich L, Tramblay Y, Saaidi A, Gascoin S, Martin E, et al. Present and future high-resolution climate forcings over semiarid catchments: case of the tensift (Morocco). Atmosphere. 2021;12(3):370. https://doi.org/10.3390/atmos12030370

50. Twine TE, Kustas WP, Norman JM, Cook DR, Houser PR, Meyers TP. Correcting eddy-covariance flux underestimates over a grassland. Agri For Meteorol. 2000.

51. Er-Raki S, Chehbouni A, Guemouria N, Duchemin B, Ezzahar J, Hadria R. Combining FAO-56 model and ground-based remote sensing to estimate water consumptions of wheat crops in a semi-arid region. Agri Water Manag. 2007;87(1):41–54. https://doi.org/10.1016/j.agwat.2006.02.004

52. Duchemin B, Hadria R, Erraki S, Boulet G, Maisongrande P, Chehbouni A, et al. Monitoring wheat phenology and irrigation in Central Morocco: on the use of relationships between evapotranspiration, crops coefficients, leaf area index and remotely-sensed vegetation indices. Agri Water Manag. 2006;79(1):1–27. https://doi.org/10.1016/j.agwat.2005.02.013

53. Belaqziz S, Mangiarotti S, Le Page M, Khabba S, Er-Raki S, Agouti T. Irrigation scheduling of a classical gravity network based on the covariance matrix adaptation - evolutionary strategy algorithm. Comput Electron Agric. 2014;102:64–72.

54. Aouade G, Jarlan L, Ezzahar J, Er-Raki S, Napoly A, Benkaddour A, et al. Evapotranspiration partition using the multiple energy balance version of the ISBA-A-g<;sub>;s<;/sub>; land surface model over two irrigated crops in a semi-arid Mediterranean region (Marrakech, Morocco). Hydrol Earth Syst Sci. 2020;24(7):3789–814. https://doi.org/10.5194/hess-24-3789-2020

55. Diarra A, Jarlan L, Er-Raki S, Le Page M, Aouade G, Tavernier A, et al. Performance of the two-source energy budget (TSEB) model for the monitoring of evapotranspiration over irrigated annual crops in North Africa. Agric Water Manag. 2017;193:71–88. https://doi.org/10.1016/j.agwat.2017.08.007

56. Faroux S, Kaptué Tchuenté AT, Roujean J-L, Masson V, Martin E, Le Moigne P. ECOCLIMAP-II/Europe: a twofold database of ecosystems and surface parameters at 1 km resolution based on satellite information for use in land surface, meteorological and climate models. Geosci Model Dev. 2013;6(2):563–82. https://doi.org/10.5194/gmd-6-563-2013

57. Carrer D, Meurey C, Ceamanos X, Roujean J-L, Calvet J-C, Liu S. Dynamic mapping of snow-free vegetation and bare soil albedos at global 1km scale from 10-year analysis of MODIS satellite products. Remote Sens Environ. 2014;140:420–32. https://doi.org/10.1016/j.rse.2013.08.041

58. Munier S, Carrer D, Planque C, Camacho F, Albergel C, Calvet J-C. Satellite leaf area index: global scale analysis of the tendencies per vegetation type over the last 17 years. Remote Sens. 2018;10(3):424. https://doi.org/10.3390/rs10030424

59. Clapp RB, Hornberger GM. Empirical equations for some soil hydraulic properties. Water Resour Res. 1978;14(4):601–4. https://doi.org/10.1029/wr014i004p00601

60. Meier J, Zabel F, Mauser W. A global approach to estimate irrigated areas – a comparison between different data and statistics. Hydrol Earth Syst Sci. 2018;22(2):1119–33. https://doi.org/10.5194/hess-22-1119-2018

61. Simonneaux V, Duchemin B, Helson D, Er-Raki S, Olioso A, Chehbouni AG. The use of high-resolution image time series for crop classification and evapotranspiration estimate over an irrigated area in central Morocco. Int J Remote Sens. 2008;29(1):95–116. https://doi.org/10.1080/01431160701250390

62. Noilhan J, Planton S. A simple parameterization of land surface processes for meteorological models. 1989.

63. Noilhan J, Mahfouf J-F. The ISBA land surface parameterisation scheme. Glob PlanetChange. 1996;13(1–4):145–59. https://doi.org/10.1016/0921-8181(95)00043-7

64. Masson V, Le Moigne P, Martin E, Faroux S, Alias A, Alkama R. The surfexv7.2 land and ocean surface platform for coupled or offline simulation of earth surface variables and fluxes. Geosci Model Dev. 2013;6:929–60.

65. Calvet J-C, Noilhan J-É, Roujean J-L, Bessemoulin P, Cabelguenne M, Olioso A. An interactive vegetation SVAT model tested against data from six contrasting sites. 1998.

66. Calvet J-C. Investigating soil and atmospheric plant water stress using physiological and micrometeorological data. 2000.

67. Jacobs CMJ. Direct impact of atmospheric CO2 enrichment on regional transpiration. 1994.

68. Carrer D, Lafont S, Roujean JL, Calvet JC, Meurey C, Le Moigne P. Incoming solar and infrared radiation derived from METEOSAT: Impact on the modeled land water and energy budget over France. J Hydrometeorol. 2012;13:504–20.

69. Decharme B, Boone A, Delire C, Noilhan J. Local evaluation of the Interaction between Soil Biosphere Atmosphere soil multilayer diffusion scheme using four pedotransfer functions. J Geophys Res. 2011;116(D20). https://doi.org/10.1029/2011jd016002

70. Decharme B, Martin E, Faroux S. Reconciling soil thermal and hydrological lower boundary conditions in land surface models. JGR Atmospheres. 2013;118(14):7819–34. https://doi.org/10.1002/jgrd.50631

71. Garrigues S, Olioso A, Calvet JC, Martin E, Lafont S, Moulin S, et al. Evaluation of land surface model simulations of evapotranspiration over a 12-year crop succession: impact of soil hydraulic and vegetation properties. Hydrol Earth Syst Sci. 2015;19(7):3109–31. https://doi.org/10.5194/hess-19-3109-2015

72. Deardorff JW. Efficient prediction of ground surface temperature and moisture, with inclusion of a layer of vegetation. J Geophys Res. 1978;83(C4):1889–903. https://doi.org/10.1029/jc083ic04p01889

73. Nachtergaele F, Van Velthuizen H, Verelst L. Harmonized World Soil Database - Version 1.1. FAO. 2009; p. 43.

74. Allen RG, Pereira LS. Crop evapotranspiration: guidelines for computing crop water requirements. 1998.

75. le Polain de Waroux Y, Lambin EF. Monitoring degradation in arid and semi-arid forests and woodlands: The case of the argan woodlands (Morocco). Appl Geogr. 2012;32(2):777–86. https://doi.org/10.1016/j.apgeog.2011.08.005

76. Levidow D, Zaccaria R, Maia E, Vivas M, Todorovic A, Scardigno A. Agricultural water management. Agric Water Manag. 2014;146(C):84–94.

77. Jarlan L, Khabba S, Szczypta C, Lili-Chabaane Z, Driouech F, Le Page M et al. Water resources in South Mediterranean catchments: assessing climatic drivers and impacts. In: par S, Thiébault et JP Moatti édité. The mediterranean region under climate change. Paris; 2016. p. 303–9.

78. Nassah H, Er-Raki S, Khabba S, Fakir Y, Raibi F, Merlin O. Evaluation and analysis of deep percolation losses of drip irrigated citrus crops under non-saline and saline conditions in a semi-arid area. Biosyst Eng. 2018;165:10–24.

79. Khabba S, Jarlan L, Er-Raki S, Le Page M, Ezzahar J, Boulet G. The sudmed program and the joint international laboratory TREMA: a decade of water transfer study in the soil-plant-atmosphere system over irrigated crops in semi-arid area. Procedia Environ Sci. 2013;19:524–33.

80. Benouniche M, Kuper M, Hammani A, Boesveld H. Making the user visible: analysing irrigation practices and farmers' logic to explain actual drip irrigation performance. Irrig Sci. 2014;32:405–20.

81. Massari C, Modanesi S, Dari J, Gruber A, De Lannoy GJM, Girotto M, et al. A Review of irrigation information retrievals from space and their utility for users. Remote Sens. 2021;13(20):4112. https://doi.org/10.3390/rs13204112

82. Ouaadi N, Jarlan L, Khabba S, Ezzahar J, Le Page M, Merlin O. Irrigation amounts and timing retrieval through data assimilation of surface soil moisture into the FAO-56 approach in the south mediterranean region. Remote Sens. 2021;13(14):2667. https://doi.org/10.3390/rs13142667

83. Le Page M. Une contribution pour l'utilisation de la télédétection spatiale à la gestion de l'eau agricole. PhD Manuscript. 2020;165.

84. Brocca L, Tarpanelli A, Filippucci P, Dorigo W, Zaussinger F, Gruber A, et al. How much water is used for irrigation? A new approach exploiting coarse resolution satellite soil moisture products. Int J Appl Earth Obs Geoinf. 2018;73:752–66. https://doi.org/10.1016/j.jag.2018.08.023

85. Olivera-Guerra L, Merlin O, Er-Raki S. Irrigation retrieval from Landsat optical/thermal data integrated into a crop water balance model: a case study over winter wheat fields in a semi-arid region. Remote Sens Environ. 2020;239:111627. https://doi.org/10.1016/j.rse.2019.111627

86. Markovich KH, Manning AH, Condon LE, McIntosh JC. Mountain-block recharge: A review of current understanding. Water Resour Res. 2019;55:8278–304.

87. Wilson JL, Guan H. Mountain-block hydrology and mountain-front recharge. Groundwater Recharge in a Desert Environment: The Southwestern United States. 2004;113–37.

88. Shanafield M, Cook PG. Transmission losses, infiltration and groundwater recharge through ephemeral and intermittent streambeds: a review of applied methods. J Hydrol. 2014;511:518–29.

89. Kamal S, Sefiani S, Laftouhi N-E, El Mandour A, Moustadraf J, Elgettafi M, et al. Hydrochemical and isotopic assessment for characterizing groundwater quality and recharge processes under a semi arid area: Case of the Haouz plain aquifer (Central Morocco). J Afr Earth Sci. 2021;174:104077. https://doi.org/10.1016/j.jafrearsci.2020.104077

90. Hajhouji Y, Fakir Y, Gascoin S, Simonneaux V, Chehbouni A. Dynamics of groundwater recharge near a semi-arid Mediterranean intermittent stream under wet and normal climate conditions. J Arid Land. 2022;14(7):739–52. https://doi.org/10.1007/s40333-022-0067-z

91. Bouimouass H, Fakir Y, Tweed S, Leblanc M. Groundwater recharge sources in semiarid irrigated mountain fronts. Hydrol Earth Syst Sci. 2020;34:1598–615.

92. Marchane A, Tramblay Y, Hanich L, Ruelland D, Jarlan L. Climate change impacts on surface water resources in the Rheraya catchment (High Atlas, Morocco). Hydrol Sci J. 2017;62(6):979–95. https://doi.org/10.1080/02626667.2017.1283042

93. Schmandt J, Kibaroglu A, Buono R, Thomas S, . Sustainability of engineered rivers in arid lands. 2021. https://doi.org/10.1017/9781108261142

94. Kuper M, Ameur F, Hammani A. Unraveling the enduring paradox of increased pressure on groundwater through efficient drip irrigation. In: Drip Irrigation for Agriculture: Untold Stories of Efficiency, Innovation and Development. 2017. https://doi.org/10.4324/9781315537146

95. Molle F, Tanouti O. Squaring the circle: Agricultural intensification vs. water conservation in Morocco. Agric Water Manag. 2017;192:170–9. https://doi.org/10.1016/j.agwat.2017.07.009

96. Grafton RQ, Williams J, Perry CJ, Molle F, Ringler C, Steduto P, et al. The paradox of irrigation efficiency. Sci. 2018;361(6404):748–50. https://doi.org/10.1126/science.aat9314 PMID: 30139857

97. O'Leary GJ, Christy B, Nuttall J, Huth N, Cammarano D, Stöckle C, et al. Response of wheat growth, grain yield and water use to elevated CO2 under a Free-Air CO2 Enrichment (FACE) experiment and modelling in a semi-arid environment. Glob Chang Biol. 2015;21(7):2670–86. https://doi.org/10.1111/gcb.12830 PMID: 25482824

98. Drake BG, Gonzàlez-Meler MA, Long SP. More efficient plants: A consequence of rising atmospheric CO2?. Annu Rev Plant Biol. 1997;48.

99. Mearns LO, Rosenzweig C, Goldberg R. Mean and variance change in climate scenarios: methods, agricultural application and measurement of uncertainty. Clim Change. 1997;35:367–96.